Three-dimensional elasticity solution for bending of transversely isotropic functionally graded plates

B. Woodward, M. Kashtalyan

Accepted Manuscript

Title: Three-dimensional elasticity solution for bending of transversely isotropic functionally graded plates

Authors: B. Woodward, M. Kashtalyan

PII: S0997-7538(11)00049-0

DOI: 10.1016/j.euromechsol.2011.04.003

Reference: EJMSOL 2701

To appear in: *European Journal of Mechanics / A Solids*

Received Date: 29 September 2010

Revised Date: 25 March 2011

Accepted Date: 7 April 2011

Please cite this article as: Woodward, B., Kashtalyan, M. Three-dimensional elasticity solution for bending of transversely isotropic functionally graded plates, European Journal of Mechanics / A Solids (2011), doi: 10.1016/j.euromechsol.2011.04.003

THREE-DIMENSIONAL ELASTICITY SOLUTION FOR BENDING OF TRANSVERSELY ISOTROPIC FUNCTIONALLY GRADED PLATES

B. Woodward, M. Kashtalyan*

Centre for Micro- and Nanomechanics (CEMINACS),

School of Engineering, University of Aberdeen, AB24 3UE, Scotland, UK

ABSTRACT

This paper presents a three-dimensional elasticity solution for a simply supported, transversely isotropic functionally graded plate subjected to transverse loading, with Young's moduli and the shear modulus varying exponentially through the thickness and Poisson's ratios being constant. The approach makes use of the recently developed displacement functions for inhomogeneous transversely isotropic media. Dependence of stress and displacement fields in the plate on the inhomogeneity ratio, geometry and degree of anisotropy is examined and discussed. The developed three-dimensional solution for transversely isotropic functionally graded plate is validated through comparison with the available three-dimensional solutions for isotropic functionally graded plates, as well as the classical and higher-order plate theories.

Keywords: Functionally graded material; Transversely isotropic; Three-dimensional analytical solution; Rectangular plate; Displacement potential functions

* Corresponding author, e-mail: m.kashtalyan@abdn.ac.uk, tel/fax: +44(0)1224 272519

1. Introduction

Functionally graded materials (FGMs) are a type of heterogeneous composite materials exhibiting gradual variation in volume fraction of their constituents from one surface of the material to the other, resulting in properties which vary continuously across the material. These materials were initially developed in the 1980s for use in high temperature applications by Japanese scientists, who showed that the FGMs provide heat and corrosion resistance whilst retaining strength and toughness (Yamanouchi et al., 1990; Koizumi, 1993).

Since then a large amount of research has been undertaken into their performance and production (Suresh and Mortensen, 1998; Miyamoto et al., 1999) and as such their use has become far more widespread, with current applications including dental implants, heat exchanger tubes, engine components and to eliminate mismatch of thermal properties in metal and ceramic bonding.

Theoretical modelling of functionally graded plates remains an active research area (Birman and Bird, 2007), with the development of analytical elasticity solutions being of particular importance.

Bian et al (2005) have developed a plate theory for a simply supported functionally graded plate under cylindrical bending utilising shape functions to describe inhomogeneity in the transverse direction. These results are then compared with those found using first and third order shear deformation plate theories. The paper however only covers a one-dimensional problem.

The response of a functionally graded plate to transverse uniform load was investigated analytically by Zenkour (2006). Through use of generalised shear deformation theory a stress analysis is presented for an isotropic functionally graded plate with power law distribution in gradient. Comparisons are then made with an equivalent homogeneous isotropic plate.

Shariat and Eslami (2007) performed buckling analysis of rectangular functionally graded plates with linear through thickness variation of properties. Equilibrium equations are derived using third order shear deformation theory and a buckling analysis is carried out for a variety of mechanical and thermal load types.

Through use of displacement functions, Kashtalyan (2004) developed an exact three dimensional elasticity solution for the bending of functionally graded plates. The material was assumed to be isotropic with exponential variation of Young's modulus through the thickness. This solution was validated through comparison with results for isotropic homogeneous plate and has become a benchmark solution used by other researchers (Abrate, 2008; Zhong and Shang, 2008; Brischetto, 2009; Yunet et al., 2010).

A three-dimensional elasticity solution for exponentially graded rectangular plate of variable thickness was developed by Xu and Zhou (2009), while axisymmetric bending of functionally graded isotropic circular plates was investigated by Zheng and Zhong (2009) and Wang et al (2010).

Compared to isotropic functionally graded plates, transversely isotropic plates with gradient in elastic properties have received considerably less attention in the literature.

An exact three dimensional analysis for a simply supported functionally graded piezoelectric plate with exponential variation of properties through the thickness was presented by Zhong and Shang (2003). Using the state space approach, numerical results were obtained for four different cases of sinusoidal loading.

A method of solution for stresses and displacements within a transversely isotropic functionally graded circular plate, whose elastic constants are arbitrary functions of the thickness coordinate, was described by Li et al. (2008).The loading considered was a transverse uniform load and it was shown that the stresses and displacements through the

thickness of the plate could be controlled through selection and optimization of the five engineering constants. This solution is however only valid for circular FGM plates under one specific type of loading. The authors concluded that there is still significant research required to model other types of axisymmetric loading.

Yun et al. (2010) provided an analytical solution for the axisymmetric bending of transversely isotropic functionally graded circular plates subject to arbitrarily transverse loads using the direct displacement method. Verification is then carried out through comparison with a finite element model.

In this paper an approach utilising displacement functions for inhomogeneous transversely isotropic media developed by Kashtalyan and Rushchitsky (2009) allows an exact three dimensional elasticity solution for functionally graded transversely isotropic rectangular plate to be developed. It is assumed that the material has constant Poisson's ratios and that Young's and shear moduli vary exponentially through the thickness.

2. Problem formulation

The plate under consideration, with length a, width b and thickness h, is shown relative to the $x_1x_2x_3$ Cartesian coordinates in Figure 1.

The plate is assumed to be simply supported on the edges such that

$$x_1 = 0, a: \quad \sigma_{11} = 0, \quad u_2 = u_3 = 0, \tag{1a}$$

$$x_2 = 0, b: \quad \sigma_{22} = 0, \quad u_1 = u_3 = 0, \tag{1b}$$

where σ_{ij} are the components of the stress tensor and u_i are the components of the displacement vector.

The loading is applied transversely and provides the final six boundary conditions. Since it is applied at the upper surface, $x_3 = h$, it can be written that

$$\sigma_{33} = Q(x_1, x_2), \quad \sigma_{13} = \sigma_{23} = 0 \tag{2a}$$

$$Q(x_1, x_2) = -q_{mn} \sin\frac{\pi m x_1}{a} \sin\frac{\pi n x_2}{b} \tag{2b}$$

where q_{mn} is the amplitude of the loading. The bottom surface, $x_3 = 0$ is load-free, i.e.

$$\sigma_{33} = \sigma_{13} = \sigma_{23} = 0 \tag{2c}$$

The material of the plate material is an inhomogeneous transversely isotropic with the x_3-axis as an axis of material symmetry. Hence the following constitutive equations can be written

$$\sigma_{11} = c_{11}\varepsilon_{11} + c_{12}\varepsilon_{22} + c_{13}\varepsilon_{33} \tag{3a}$$

$$\sigma_{22} = c_{12}\varepsilon_{11} + c_{11}\varepsilon_{22} + c_{13}\varepsilon_{33} \tag{3b}$$

$$\sigma_{33} = c_{13}\varepsilon_{11} + c_{13}\varepsilon_{22} + c_{33}\varepsilon_{33} \tag{3c}$$

$$\sigma_{23} = 2c_{44}\varepsilon_{23} \tag{3d}$$

$$\sigma_{13} = 2c_{44}\varepsilon_{13} \tag{3e}$$

$$\sigma_{12} = 2c_{66}\varepsilon_{12} = (c_{11} - c_{12})\varepsilon_{12} \tag{3f}$$

where ε_{ij} are the components of the strain tensor and $c_{11}, c_{12}, c_{13}, c_{33}, c_{44}$ are five independent elastic coefficients, which in the general case depend on x_1, x_2, x_3.

Let E, ν and $G = \dfrac{E}{2(1+\nu)}$ denote the Young's modulus, Poisson's ratio and shear modulus in the plane of isotropy (i.e. any plane normal to the x_3-axis), and E', ν' and G' the Young's modulus, Poisson's ratio and shear modulus in any plane normal to the plane of isotropy.

It is assumed that:

(i) Poisson's ratios ν, ν' are constant, i.e.

$$\nu = const, \quad \nu' = const \tag{4a}$$

(ii) Young's moduli E and E' and the shear modulus G', have the same functional dependence on the co-ordinate x_3, i.e.

$$E(x_3) = E_0 m(x_3), \qquad E_0 = const \tag{4b}$$

$$E'(x_3) = E_0' m(x_3), \qquad E_0' = const \tag{4c}$$

$$G'(x_3) = G_0' m(x_3), \qquad G_0' = const \tag{4d}$$

where $m = m(x_3)$, henceforth termed the inhomogeneity function, is a sufficiently smooth function of the transverse co-ordinate x_3. It follows that the elastic coefficients $c_{11}, c_{12}, c_{13}, c_{33}, c_{44}$ also have the same functional dependence on the transverse co-ordinate x_3. Hence:

$$c_{11}(x_3) = c_{11}^0 m(x_3) \tag{5a}$$

$$c_{12}(x_3) = c_{12}^0 m(x_3) \tag{5b}$$

$$c_{13}(x_3) = c_{13}^0 m(x_3) \tag{5c}$$

$$c_{33}(x_3) = c_{33}^0 m(x_3) \tag{5d}$$

$$c_{44}(x_3) = c_{44}^0 m(x_3) \tag{5e}$$

where

$$c_{11}^0 = \frac{1-(\nu')^2(E_0/E_0')}{1-\nu^2+(1+2\nu)(\nu')^2(E_0/E_0')} E_0 \tag{5f}$$

$$c_{12}^0 = \frac{\nu-(\nu')^2(E_0/E_0')}{1-\nu^2+(1+2\nu)(\nu')^2(E_0/E_0')} E_0 \tag{5g}$$

$$c_{13}^0 = \frac{\nu'(1-\nu)}{1-\nu^2+(1+2\nu)(\nu')^2(E_0/E_0')} E_0 \tag{5h}$$

$$c_{33}^0 = \frac{1-\nu^2}{1-\nu^2+(1+2\nu)(\nu')^2(E_0/E_0')} E_0' \tag{5i}$$

$$c_{44}^0 = G_0' \tag{5j}$$

In the absence of body forces, the equilibrium equations for inhomogeneous transversely isotropic plate are

$$\frac{\partial \sigma_{11}}{\partial x_1} + \frac{\partial \sigma_{12}}{\partial x_2} + \frac{\partial \sigma_{13}}{\partial x_3} = 0 \tag{6a}$$

$$\frac{\partial \sigma_{12}}{\partial x_1}+\frac{\partial \sigma_{22}}{\partial x_2}+\frac{\partial \sigma_{23}}{\partial x_3}=0 \tag{6b}$$

$$\frac{\partial \sigma_{13}}{\partial x_1}+\frac{\partial \sigma_{23}}{\partial x_2}+\frac{\partial \sigma_{33}}{\partial x_3}=0 \tag{6c}$$

Using strain – displacement relations

$$\varepsilon_{ij}=\frac{1}{2}\left(\frac{\partial u_i}{\partial x_j}+\frac{\partial u_j}{\partial x_i}\right) \tag{7}$$

and the constitutive equations (3), the equilibrium equations (6) can be re-written in terms of displacements (Kashtalyan and Rushchitsky, 2009) as

$$(c_{11}-c_{12})\Delta_{3g}u_1+2\frac{\partial e}{\partial x_1}+2\frac{\partial c_{44}}{\partial x_3}\left(\frac{\partial u_1}{\partial x_3}+\frac{\partial u_3}{\partial x_1}\right)=0 \tag{8a}$$

$$(c_{11}-c_{12})\Delta_{3g}u_2+2\frac{\partial e}{\partial x_2}+2\frac{\partial c_{44}}{\partial x_3}\left(\frac{\partial u_2}{\partial x_3}+\frac{\partial u_3}{\partial x_2}\right)=0 \tag{8b}$$

$$c_{44}\Delta_{3/g}u_3+e_3'+\frac{\partial c_{13}}{\partial x_3}\left(\frac{\partial u_1}{\partial x_1}+\frac{\partial u_2}{\partial x_2}\right)+\frac{\partial c_{33}}{\partial x_3}\frac{\partial u_3}{\partial x_3}=0 \tag{8c}$$

where

$$e=\frac{1}{2}(c_{11}+c_{12})\frac{\partial u_1}{\partial x_1}+\frac{1}{2}(c_{11}+c_{12})\frac{\partial u_2}{\partial x_2}+(c_{44}+c_{13})\frac{\partial u_3}{\partial x_3} \tag{8d}$$

$$e_3'=(c_{44}+c_{13})\frac{\partial^2 u_1}{\partial x_1\partial x_3}+(c_{44}+c_{13})\frac{\partial^2 u_2}{\partial x_2\partial x_3}+\left(c_{33}-\frac{c_{11}-c_{12}}{2}\right)\frac{\partial^2 u_3}{\partial^2 x_3} \tag{8e}$$

$$\Delta_{3g}=\Delta_2+g^o\frac{\partial^2}{\partial x_3^2},\quad \Delta_{3/g}=\Delta_2+\frac{1}{g^o}\frac{\partial^2}{\partial x_3^2} \tag{8f,g}$$

$$\Delta_2=\frac{\partial^2}{\partial x_1^2}+\frac{\partial^2}{\partial x_2^2},\qquad g=\frac{2c_{44}}{c_{11}-c_{12}}=\frac{2c_{44}^o}{c_{11}^o-c_{12}^o}=g^o=const \tag{8h,i}$$

Constant g^o represents the ratio between the shear moduli in a plane of isotropy and a plane normal to it. For isotropic materials it is equal to unity, for transversely isotropic materials it can be used to characterise the degree of anisotropy exhibited by the material.

It was shown by Kashtalyan and Rushchitsky (2009) that the displacement vector can be represented in terms of two displacement functions Φ and Ψ as

$$u_1 = \frac{\partial \Phi}{\partial x_2} - \left[\frac{c_{13}}{c_{11}c_{33} - c_{13}^2} \Delta_2 - \frac{c_{33}}{c_{11}c_{33} - c_{13}^2} \frac{\partial^2}{\partial x_3^2} \right] \frac{\partial \Psi}{\partial x_1} \tag{9a}$$

$$u_2 = -\frac{\partial \Phi}{\partial x_1} - \left[\frac{c_{13}}{c_{11}c_{33} - c_{13}^2} \Delta_2 - \frac{c_{33}}{c_{11}c_{33} - c_{13}^2} \frac{\partial^2}{\partial x_3^2} \right] \frac{\partial \Psi}{\partial x_2} \tag{9b}$$

$$u_3 = -\frac{1}{c_{44}} \Delta_2 \frac{\partial \Psi}{\partial x_3} + \frac{\partial}{\partial x_3} \left[\frac{c_{13}}{c_{11}c_{33} - c_{13}^2} \Delta_2 - \frac{c_{33}}{c_{11}c_{33} - c_{13}^2} \frac{\partial^2}{\partial x_3^2} \right] \Psi \tag{9c}$$

From equations (9a-c), strain – displacement relations (7) and constitutive equations (3), components of the stress tensor can be expressed in terms of functions Φ and Ψ (derivation is outlined in appendix A)

$$\sigma_{11} = \left[\left(\frac{c_{11}c_{13} - c_{12}c_{13}}{c_{11}c_{33} - c_{13}^2} \Delta_2 + \frac{c_{12}c_{33} - c_{13}^2}{c_{11}c_{33} - c_{13}^2} \frac{\partial^2}{\partial x_3^2} \right) \frac{\partial^2}{\partial x_2^2} + \frac{\partial^4}{\partial x_1^2 \partial x_3^2} \right] \Psi + (c_{11} - c_{12}) \frac{\partial^2 \Phi}{\partial x_1 \partial x_2} \tag{9d}$$

$$\sigma_{22} = \left[\left(\frac{c_{11}c_{13} - c_{12}c_{13}}{c_{11}c_{33} - c_{13}^2} \Delta_2 + \frac{c_{12}c_{33} - c_{13}^2}{c_{11}c_{33} - c_{13}^2} \frac{\partial^2}{\partial x_3^2} \right) \frac{\partial^2}{\partial x_1^2} + \frac{\partial^4}{\partial x_2^2 \partial x_3^2} \right] \Psi - (c_{11} - c_{12}) \frac{\partial^2 \Phi}{\partial x_1 \partial x_2} \tag{9e}$$

$$\sigma_{33} = \Delta_2 \Delta_2 \Psi \tag{9f}$$

$$\sigma_{12} = \frac{c_{12} - c_{11}}{c_{11}c_{33} - c_{13}^2} \left(c_{13} \Delta_2 - c_{33} \frac{\partial^2}{\partial x_3^2} \right) \frac{\partial^2 \Psi}{\partial x_1 \partial x_2} - \frac{c_{11} - c_{12}}{2} \left(\frac{\partial^2}{\partial x_1^2} - \frac{\partial^2}{\partial x_2^2} \right) \Phi \tag{9g}$$

$$\sigma_{13} = -\Delta_2 \frac{\partial^2 \Psi}{\partial x_1 \partial x_3} + c_{44} \frac{\partial^2 \Phi}{\partial x_2 \partial x_3} \tag{9h}$$

$$\sigma_{23} = -\Delta_2 \frac{\partial^2 \Psi}{\partial x_2 \partial x_3} - c_{44} \frac{\partial^2 \Phi}{\partial x_1 \partial x_3} \tag{9i}$$

Functions Φ and Ψ satisfy the following differential equations (Kashtalyan and Rushchitsky 2009)

$$m(x_3) \Delta_2 \Phi + g^0 \frac{\partial}{\partial x_3} \left[m(x_3) \frac{\partial \Phi}{\partial x_3} \right] = 0 \tag{10a}$$

$$c_{11}^0\Delta_2\Delta_2\Psi - c_{13}^0\Delta_2\frac{\partial^2\Psi}{\partial x_3^2} + \left(c_{11}^0 c_{33}^0 - c_{13}^{0\,2}\right)m(x_3)$$
$$\times\left\{\frac{1}{c_{44}^0}\frac{\partial}{\partial x_3}\left[m^{-1}(x_3)\Delta_2\frac{\partial\Psi}{\partial x_3}\right] + \frac{c_{33}^0}{c_{11}^0 c_{33}^0 - c_{13}^{0\,2}}\frac{\partial^2}{\partial x_3}\left[m^{-1}(x_3)\frac{\partial^2\Psi}{\partial x_3^2}\right]\right. \tag{10b}$$
$$\left. - \frac{c_{13}^0}{c_{11}^0 c_{33}^0 - c_{13}^{0\,2}}\frac{\partial^2}{\partial x_3}\left[m^{-1}(x_3)\Delta_2\Psi\right]\right\} = 0$$

subject to boundary conditions (1) and (2).

3. Separation of variable

Solution of equations (10) starts with separating variables in the displacement functions in the form

$$\Phi(x_1, x_2, x_3) = \bar{\bar{\Phi}}(x_1, x_2)\bar{\Phi}(x_3) \tag{11a}$$

$$\Psi(x_1, x_2, x_3) = \bar{\bar{\Psi}}(x_1, x_2)\bar{\Psi}(x_3) \tag{11b}$$

Substitution of these expressions into equations (10a) and (10b) allows the following four differential equations to be derived

$$\Delta_2\bar{\bar{\Phi}} + k_\Phi^2\bar{\bar{\Phi}} = 0 \tag{12a}$$

$$\Delta_2\bar{\bar{\Psi}} + k_\Psi^2\bar{\bar{\Psi}} = 0 \tag{12b}$$

$$\left[\frac{d^2}{dx_3^2} + \frac{m'(x_3)}{m(x_3)}\frac{d}{dx_3} - \frac{k_\Phi^2}{g^0}\right]\bar{\Phi} = 0 \tag{12c}$$

$$m(x_3)\frac{d^2}{dx_3}\left[m^{-1}(x_3)\frac{d^2\bar{\Psi}}{dx_3^2}\right] + \frac{c_{13}^0}{c_{33}^0}k_\Psi^2 m(x_3)\frac{d^2}{dx_3^2}\left[m^{-1}(x_3)\bar{\Psi}\right]$$
$$- \frac{c_{11}^0 c_{33}^0 - c_{13}^{0^2}}{c_{33}^0 c_{44}^0}k_\Psi^2 m(x_3)\frac{d}{dx_3}\left[m^{-1}(x_3)\frac{d\bar{\Psi}}{dx_3}\right] + \frac{c_{13}^0}{c_{33}^0}k_\Psi^2\frac{d^2\bar{\Psi}}{dx_3^2} + \frac{c_{11}^0}{c_{33}^0}k_\Psi^4\bar{\Psi} = 0 \tag{12d}$$

For a simply supported plate subjected to sinusoidal loading, with the boundary conditions described by equations (1) and (2), functions $\bar{\bar{\Phi}} = \bar{\bar{\Phi}}(x_1, x_2)$ and $\bar{\bar{\Psi}} = \bar{\bar{\Psi}}(x_1, x_2)$ can be chosen as

$$\bar{\bar{\Phi}}(x_1, x_2) = \cos\frac{\pi m x_1}{a}\cos\frac{\pi n x_2}{b} \tag{13a}$$

$$\bar{\bar{\Psi}}(x_1, x_2) = \sin\frac{\pi m x_1}{a}\sin\frac{\pi n x_2}{b} \tag{13b}$$

Then the boundary conditions on the edges of the plate are satisfied exactly.

Selecting the inhomogeneity function such that it is an exponential one,

$$m(x_3) = \exp\frac{\alpha x_3}{h} \tag{14}$$

and non-dimensionalising reduce equations (12c) and (12d) to the following second- and fourth-order differential equations with constant coefficients

$$h^2\frac{d^2\bar{\Phi}}{dx_3^2} + \alpha h\frac{d\bar{\Phi}}{dx_3} - \frac{k_\Phi^2 h^2}{g^0}\bar{\Phi} = 0 \tag{15a}$$

$$\begin{aligned} &h^4\frac{d^4\bar{\Psi}}{dx_3^4} - 2\alpha h^3\frac{d^3\bar{\Psi}}{dx_3^3} + h^2\left[\alpha^2 + \left(2\frac{c_{13}^0}{c_{33}^0} - \frac{c_{11}^0 c_{33}^0 - c_{13}^{0\,2}}{c_{33}^0 c_{44}^0}\right)k_\Psi^2 h^2\right]\frac{d^2\bar{\Psi}}{dx_3^2} \\ &-\alpha k_\Psi^2 h^3\left[2\frac{c_{13}^0}{c_{33}^0} - \frac{c_{11}^0 c_{33}^0 - c_{13}^{0\,2}}{c_{33}^0 c_{44}^0}\right]\frac{d\bar{\Psi}}{dx_3} + \frac{k_\Psi^2 h^2\left(c_{11}^0 k_\Psi^2 h^2 + c_{13}^0\alpha^2\right)}{c_{33}^0}\bar{\Psi} = 0 \end{aligned} \tag{15b}$$

where

$$k_\Phi^2 = k_\Psi^2 = \pi^2\left[\left(\frac{m}{a}\right)^2 + \left(\frac{n}{b}\right)^2\right] \tag{15c}$$

It is worth mentioning that the exponential variation of material properties with transverse co-ordinate has been used by a number of researchers investigating functionally graded materials, in particular Jin and Batra (1996), Gu and Asaro (1997), Sankar (2001), Anderson (2003), Kashtalyan and Menshykova (2007, 2009a,b), and Woodward and Kashtalyan (2010).

The solutions to equations (15a) and (15b) will vary depending on the values of the elastic constants and parameters k_Φ and k_Ψ. Their solution is detailed in appendix B.

If the discriminant of the characteristic equation corresponding to equation (15b) is negative then

$$\bar{\Psi} = h^4 \exp\left(\frac{\alpha x_3}{2h}\right)\left[A_1 \cosh\frac{\lambda x_3}{h}\cos\frac{\mu x_3}{h} + A_2 \cosh\frac{\lambda x_3}{h}\sin\frac{\mu x_3}{h} + A_3 \sinh\frac{\lambda x_3}{h}\cos\frac{\mu x_3}{h} + A_4 \sinh\frac{\lambda x_3}{h}\sin\frac{\mu x_3}{h}\right] \tag{16a}$$

where λ and μ are

$$\lambda = \frac{1}{4}\left[8\left(-\frac{c_{13}^0}{c_{33}^0}+\frac{1}{2}\frac{c_{11}^0}{c_{44}^0}-\frac{1}{2}\frac{c_{13}^{0^2}}{c_{33}^0 c_{44}^0}\right)k_\Psi^2 h^2 + 2\alpha^2 + 4\left(2\alpha^2 h^2 k_\Psi^2 \frac{c_{13}^0}{c_{33}^0} + \alpha^2 h^2 k_\Psi^2 \frac{c_{11}^0}{c_{44}^0} - \alpha^2 h^2 k_\Psi^2 \frac{c_{13}^{0^2}}{c_{33}^0 c_{44}^0} + 4h^4 k_\Psi^4 \frac{c_{13}^0}{c_{33}^0} + \frac{1}{4}\alpha^4\right)^{\frac{1}{2}}\right]^{\frac{1}{2}} \tag{16b}$$

and

$$\mu = \frac{1}{4}\left[8\left(\frac{c_{13}^0}{c_{33}^0}-\frac{1}{2}\frac{c_{11}^0}{c_{44}^0}+\frac{1}{2}\frac{c_{13}^{0^2}}{c_{33}^0 c_{44}^0}\right)k_\Psi^2 h^2 - 2\alpha^2 + 4\left(2\alpha^2 h^2 k_\Psi^2 \frac{c_{13}^0}{c_{33}^0} + \alpha^2 h^2 k_\Psi^2 \frac{c_{11}^0}{c_{44}^0} - \alpha^2 h^2 k_\Psi^2 \frac{c_{13}^{0^2}}{c_{33}^0 c_{44}^0} + 4h^4 k_\Psi^4 \frac{c_{13}^0}{c_{33}^0} + \frac{1}{4}\alpha^4\right)^{\frac{1}{2}}\right]^{\frac{1}{2}} \tag{16c}$$

If the discriminant of the characteristic equation corresponding to equation (15b) is positive, function $\bar{\Psi}$ can be found following a procedure similar to that outlined in Appendix B.

The solution of second order equation (15a) yields

$$\bar{\Phi} = \frac{h^2}{c_{44}^0}\exp\left(-\frac{\alpha x_3}{2h}\right)\left[A_5 \cosh\left(\frac{\beta x_3}{h}\right) + A_6 \sinh\left(\frac{\beta x_3}{h}\right)\right] \tag{17a}$$

where

$$\beta = \sqrt{\frac{\alpha^2}{4} + k_\Phi^2 h^2 \frac{c_{11}^0 - c_{12}^0}{c_{44}^0}} \tag{17b}$$

In equations (16) – (17), A_i $(i=1,\ldots,6)$ are six arbitrary constants that can be found from the boundary conditions on top and bottom surfaces of the plate, given by equations (2a) and (2b).

Substitution of functions $\tilde{\tilde{\Phi}}$ and $\tilde{\tilde{\Psi}}$, equations (13a, b), and functions $\tilde{\Phi}$ and $\tilde{\Psi}$, equations (16, 17), into equations (11a, b) and then into equations (9), gives the following expressions for stresses and displacements in a simply supported transversely isotropic functionally graded plate under sinusoidal loading with exponential dependence of the elastic constants on the thickness co-ordinate

$$u_1 = \sum_{j=1}^{6} A_j U_{1,j}(x_3) \cos\frac{\pi m x_1}{a} \sin\frac{\pi n x_2}{b} \tag{18a}$$

$$u_2 = \sum_{j=1}^{6} A_j U_{2,j}(x_3) \sin\frac{\pi m x_1}{a} \cos\frac{\pi n x_2}{b} \tag{18b}$$

$$u_3 = \sum_{j=1}^{6} A_j U_{3,j}(x_3) \sin\frac{\pi m x_1}{a} \sin\frac{\pi n x_2}{b} \tag{18c}$$

$$\sigma_{11} = \sum_{j=1}^{6} A_j P_{11,j}(x_3) \sin\frac{\pi m x_1}{a} \sin\frac{\pi n x_2}{b} \tag{18d}$$

$$\sigma_{22} = \sum_{j=1}^{6} A_j P_{22,j}(x_3) \sin\frac{\pi m x_1}{a} \sin\frac{\pi n x_2}{b} \tag{18e}$$

$$\sigma_{33} = \sum_{j=1}^{6} A_j P_{33,j}(x_3) \sin\frac{\pi m x_1}{a} \sin\frac{\pi n x_2}{b} \tag{18f}$$

$$\sigma_{12} = \sum_{j=1}^{6} A_j P_{12,j}(x_3) \cos\frac{\pi m x_1}{a} \cos\frac{\pi n x_2}{b} \tag{18g}$$

$$\sigma_{13} = \sum_{j=1}^{6} A_j P_{13,j}(x_3) \cos\frac{\pi m x_1}{a} \sin\frac{\pi n x_2}{b} \tag{18h}$$

$$\sigma_{23} = \sum_{j=1}^{6} A_j P_{23,j}(x_3) \sin\frac{\pi m x_1}{a} \cos\frac{\pi n x_2}{b} \tag{18i}$$

Functions $U_{i,j}$ and $P_{rt,j}$ are specified in Appendix C.

4. Validation

The developed three-dimensional solution for transversely isotropic functionally graded plate is validated through comparison with the available three-dimensional solutions for isotropic functionally graded plates, as well as the classical and higher order plate theories.

Since isotropy is a particular case of transverse isotropy, the proposed solution for the transversely isotropic plate can be used to obtain the solution for the isotropic plate if the elastic coefficients are adjusted as follows

$$c_{11}=c_{33}=\frac{E(1-\nu)}{(1+\nu)(1-2\nu)}\ ,\ c_{12}=c_{13}=\frac{E\nu}{(1+\nu)(1-2\nu)},\ c_{44}=G\,,\ G=\frac{E}{2(1+\nu)} \tag{19a}$$

with

$$\frac{c_{11}c_{13}-c_{12}c_{13}}{c_{11}c_{33}-c_{13}^2}=\frac{c_{12}c_{33}-c_{13}^2}{c_{11}c_{33}-c_{13}^2}=\nu\,,\qquad c_{11}-c_{12}=2G \tag{19b}$$

Upon substitution of (19a) and (19b), the expressions representing displacements and stresses in the transversely isotropic functionally graded plate, equations (9) and (18), fully coincide with the corresponding expressions for displacements and stresses for isotropic graded plate obtained by Kashtalyan (2004). Table 1 shows numerical results for the normalised displacements $\overline{u}_i=\frac{c_{44}^0 u_i}{q_{11}h}$ and stresses $\overline{\sigma}_{ij}=\sigma_{ij}/q_{11}$ obtained through use of equations (18) and (19) of the present paper. It can be seen that they are within 0.001% of those obtained by Kashtalyan (2004).

Table 2 shows normalised mid-plane displacements $\overline{u}_i=\frac{G_2 u_i}{q_{11}h}$ at the centre of a square $(a=b)$ isotropic graded plate with exponential variation of the shear modulus through the thickness based on the present 3-D solution and a thin plate theory of Chi and Chung (2006). The shear modulus varies from G_1, the value at the bottom surface of the plate, to G_2, the value at the top surface. The plate is simply supported on its edges and loaded by transverse loading $Q(x_1,x_2)=-q_{11}\sin(\pi x_1/a)\sin(\pi x_2/b)$ at the top surface. The results

are given for $G_2/G_1 = 10$ and the thickness-to-length ratio that varies from $h/a = 0.001$ (very thin plate) to $h/a = 0.2$ (moderately thick plate). The thin plate theory appears to be in good agreement with the present solution for $h/a \le 0.1$ as expected.

Table 3 shows normalised displacements $\bar{u}_i = \dfrac{G_2 u_i}{q_{11} h}$ in a very thin square isotropic graded plate with $h/a = h/b = 0.01$ for a range of shear modulus ratios G_2/G_1. Good agreement between the present 3-D solution and thin plate theory predictions is observed for all considered values of G_2/G_1.

Table 4 shows normalised mid-plane displacement $\bar{u}_3 = \dfrac{10 E_0 h^3 u_3}{a^4 q_{11}}$ at the centre of the isotropic graded plate predicted by the 3-D elasticity solution developed in this paper and two plate theories: the higher-order shear deformation plate theory (HPT) and the trigonometric shear deformation plate theory (TPT) developed by Zenkour (2007). The plate is loaded by transverse loading $Q(x_1, x_2) = -q_{11}\sin(\pi x_1/a)\sin(\pi x_2/b)$ at the top surface and simply supported on its edges. Young's modulus varies exponentially through the thickness from E_0 at the bottom surface to $E_0 \exp k$ at the top surface, while Poisson's ratio is $\nu = 0.3$. The results are given for square $(a/b = 1)$ and rectangular $(a/b = 1/6)$ plates with length-to-thickness ratios $a/h = 2$ and $a/h = 4$ (very thick plates), and a range of values of k. There appears to be good agreement between the present solution and TPT, with predictions based on HPT being less accurate.

4. Results and discussion

In this section, the results of parametric study into the three-dimensional elastic deformation of transversely isotropic graded plates are presented.

The effect of varying the inhomogeneity ratio α is explored first. Figures 2-6 show through thickness variation of the normalised stresses $\bar{\sigma}_{ij} = \sigma_{ij}/q_{11}$ and normalised

displacements $\bar{u}_i = \frac{c_{44}^0 u_i}{q_{11} h}$, for three different inhomogeneity ratios ($\alpha = 0, 2.3, 3$), corresponding to homogenous plate, plate with moderate inhomogeneity and plate with high inhomogeneity. The effect of this variation in inhomogeneity ratio was compared for two functionally graded plates: the first being thick plate $(a/h = b/h = 3)$ and the second thin plate $(a/h = b/h = 10)$.

The properties of the material are taken to be those of Beryl rock (Eskandari and Shodja, 2010). Its properties are defined in Table 5. As an example, a plot of the variation in constant c_{11} through the thickness of the plate is given in Figure 2.

When considering the transverse normal stress $\bar{\sigma}_{33}$ (Fig. 3A, B) it is seen that as the inhomogeneity ratio is increased at any point within the plate this stress component decreases for both thick and thin plates. Study of through thickness variation of transverse shear stress $\bar{\sigma}_{13}$ (Fig 4A, B) shows that as the inhomogeneity ratio is increased, the magnitude of this stress component increases, reaching a peak in the upper half of the plate. It can be seen once more that thick and thin plates behave in the same manner. The plots of normalised in-plane normal stress $\bar{\sigma}_{11}$ (Fig. 5A, B) and normalised in-plane shear stress $\bar{\sigma}_{12}$ (Fig. 6A, B) show that increasing the inhomogeneity ratio in both thick and thin plates causes increases in this stress component in the centre and upper sections of the plate, whilst causing a slight decrease in stress for the lower section of the plate.

Analysis of through thickness in-plane displacement $\bar{u}_1$ (Fig. 7A, B) shows that as inhomogeneity ratio increases, the additional stiffness this provides causes the magnitude of this displacement for both thick and thin plates to decreases. This plot is highly non-linear, emphasizing the need for 3D stress analysis. A similar result is seen for the

transverse displacement $\bar{u}_3$ (Fig.8A, B) with a decrease in this component for both plate geometries.

In order to further study the behaviour of transversely isotropic functionally graded plates, the effect of varying the degree of anisotropy of the material will now be considered, again using Beryl rock, which has properties as defined in Table 5. For this material the ratio of shear moduli in the plane of isotropy and the plane normal to it is 0.75. In order for a comparison to be made, constant c_{44}^0 will be varied (being set to 0.5, 2 and 10 GPa), giving three degrees of anisotropy: high anisotropy $g^0 = 0.038,$ medium anisotropy $g^0 = 0.15$ and low anisotropy $g^0 = 0.75$. The inhomogeneity ratio is now fixed as $\alpha = 2.3$. Figures 9-14 show through thickness variation of the normalised stresses $\bar{\sigma}_{ij} = \sigma_{ij} / q_{11}$ and normalised displacements $\bar{u}_i = \dfrac{c_{44}^0 u_i}{q_{11} h}$, for these three degrees of anisotropy. The effect of this variation is compared for the two plates used previously: thick plate $(a/h = b/h = 3)$ and thin plate $(a/h = b/h = 10)$.

For the cases of medium and high anisotropy, the out-of-plane normal stress $\bar{\sigma}_{33}$ (Fig. 9A, B), rises more sharply in the upper section of the thick plate, whilst having much less of an effect on the thin plates. Through thickness variation of the transverse shear stress $\bar{\sigma}_{13}$ (Fig. 10A, B), shows an increase in the stress magnitude towards the upper surface of the plate, when considering more anisotropic plates. However in the thick plate, this stress component rises to a far more pronounced peak in the upper section of the core, whilst staying almost symmetrical for the thin plate (Fig. 10B). Plots of normalised in-plane normal stress $\bar{\sigma}_{11}$ (Fig. 11A, B) and normalised in-plane shear stress $\bar{\sigma}_{12}$ (Fig. 12A, B) show for both thin and thick plates that when considering plates with higher anisotropy, the stresses in the upper half of the plate are greater, while anisotropy has far less effect on the stresses in the lower half of the plate.

Through-thickness variations of the in-plane $\bar{u}_1$ (Fig. 13A, B) and out-of-plane $\bar{u}_3$ (Fig. 14A, B) displacements show that as plate anisotropy is increased, displacements through the plate increase for both thick and thin plates. The plots of normalised in-plane displacement (Fig. 13A, B) are highly non-linear, once again emphasizing the importance of 3-D stress analysis for applications involving functionally graded materials.

5. Concluding remarks

In this paper, a three-dimensional elasticity solution for a simply supported transversely isotropic functionally graded plate subject to transverse loading has been presented. Young's moduli and the shear modulus of the material are assumed to vary exponentially through the thickness of the plate, whilst Poisson's ratios are assumed to remain constant. The solution makes use of displacement functions for inhomogeneous transversely isotropic media (Kashtalyan and Rushchitsky, 2009) and is validated through comparison with results for an isotropic functionally graded plate (Kashtalyan, 2004) as well as several plate theories.

A study of plate inhomogeneity was carried out for two plate geometries and it was seen that as the degree of inhomogeneity was increased that there are increases in most stress components in the upper half of the plate whilst a decrease was often seen in the plate centre. This was particularly the case for transverse shear stress, where under high degrees of inhomogeneity, stress concentrations can occur. Similarly when the degree of anisotropy was varied it could be seen that the greater the anisotropy of the plate, the higher the stresses in the upper half of the plate. Again under high anisotropy concentrations of transverse shear stress were found in the upper half of the plate. Many of the plots produced were highly non-linear through the thickness, showing the importance of 3-D stress analysis. It is thought that this solution can be used as benchmark for further work in the field of functionally graded transversely isotropic media.

Acknowledgements

Financial support of this research by EPSRC DTA and The Royal Society is gratefully acknowledged.

References

ABRATE, S., 2008. Functionally graded plates behave like homogeneous plates. *Composites Part B: Engineering*, **39**(1), 151-158.

ANDERSON, T.A., 2003. A 3-D elasticity solution for a sandwich composite with functionally graded core subjected to transverse loading by a rigid sphere. *Composite Structures*, **60**(3), 265-274.

BIAN, Z.G., CHEN, W.Q., LIM, C.W. and ZHANG, N., 2005. Analytical solutions for single- and multi-span functionally graded plates in cylindrical bending. *International Journal of Solids and Structures*, **42**(24-25), 6433-6456.

BIRMAN, V. and BIRD, L.W., 2007. Modelling and analysis of functionally graded materials and structures. *Applied Mechanics Reviews*, **60**(5), 195-216.

BRISCHETTO, S., 2009. Classical and mixed advanced models for sandwich plates embedding functionally graded cores. *Journal of Mechanics of Materials and Structures,* **4**(1), 13-33.

CHI, S.H. and CHUNG, Y.L., 2006. Mechanical behaviour of functionally graded material plates under transverse load - Part I: Analysis. *International Journal of Solids and Structures*, **43**(13), 3657-3674.

ESKANDARI, M. and SHODJA, H.M., 2010. Green's functions of an exponentially graded transversely isotropic half-space. *International Journal of Solids and Structures,* **47**(11-12), 1537-1545.

GU, P. and ASARO, R.J., 1997. Cracks in functionally graded materials. *International Journal of Solids and Structures,* **34**(1), 1-17.

JIN, Z. and BATRA, R.C., 1996. Interface cracking between functionally graded coatings and a substrate under antiplane shear. *International Journal of Engineering Science*, **34**(15), 1705-1716.

KASHTALYAN, M., 2004. Three-dimensional elasticity solution for bending of functionally graded rectangular plates. *European Journal of Mechanics - A/Solids,* **23**(5), 853-864.

KASHTALYAN, M. and MENSHYKOVA, M., 2009. Three-dimensional elastic deformation of a functionally graded coating/substrate system. *International Journal of Solids and Structures*, (2007), **44**(16), 5272-5288.

KASHTALYAN, M. and MENSHYKOVA, M., 2009a. Three-dimensional elasticity solution for sandwich panels with a functionally graded core. *Composite Structures*, **87**(1), 36-43.

KASHTALYAN, M. and MENSHYKOVA, M., 2009b. Effect of a functionally graded interlayer on three-dimensional elastic deformation of coated plates subjected to transverse loading. *Composite Structures*, **89**(2), 167-176.

KASHTALYAN, M. and RUSHCHITSKY, J.J., 2009. Revisiting displacement functions in three-dimensional elasticity of inhomogeneous media. *International Journal of Solids and Structures*, **46**(18-19), 3463-3470.

KOIZUMI, M., 1993. The concept of FGM. *Ceramic Transactions, Functionally Gradient Materials*, **34**, 3-10.

LI, X.Y., DING, H.J. and CHEN, W.Q., 2008. Elasticity solutions for a transversely isotropic functionally graded circular plate subject to an axisymmetric transverse load q_r^k. *International Journal of Solids and Structures*, **45**(1), 191-210.

MIYAMOTO, Y., KAYSSER, W.A., RABIN, B.H., KAWASAKI, A. and FORD, R.G., 1999. *Functionally Graded Materials: Design, Processing and Applications.* Boston, Massachusetts: Kluwer Academic Publishers.

POLYANIN, A.D. and ZAITSEV, V.F., 2003. *Handbook of Exact Solutions for Ordinary Differential Equations.* Boca Raton, Florida: Chapman & Hall.

SANKAR, B.V., 2001. An elasticity solution for functionally graded beams. *Composites Science and Technology*, **61**(5), 689-696.

SHARIAT, B.A.S. and ESLAMI, M.R., 2007. Buckling of thick functionally graded plates under mechanical and thermal loads. *Composite Structures*, **78**(3), 433-439.

SURESH, S. and MORTENSEN, A., 1998. *Fundamentals of functionally graded materials.* London: Maney.

WANG, Y., XU, R. and DING, H., 2010. Three-dimensional solutions of axisymmeric bending of functionally graded circular plates. *Composite Structures*, **92**(7), 1683-1693.

WOODWARD, B., KASHTALYAN, M., 2010. Bending response of sandwich panels with graded core: 3D elasticity analysis. *Mechanics of Advanced Materials and Structures* (2010), 17(8), 586-594.

XU, Y. and ZHOU, D., 2009. Three-dimensional elasticity solutions of functionally graded rectangular plates with variable thickness. *Composite Structures*, **91** (1), 56-65.

YAMANOUCHI, M., KOIZUMI, M., HIRAI, T. and SHIOTA, I., 1990. *Proceedings of the First International Symposium on Functionally Gradient Materials.* Sendai, Japan.

YUN, W., RONGQIAO, X. and HAOJIANG, D., 2010. Three-dimensional solution of axisymmetric bending of functionally graded circular plates. *Composite Structures,* **92**(7), 1683-1693.

ZENKOUR, A.M., 2006. Generalized shear deformation theory for bending analysis of functionally graded plates. *Applied Mathematical Modelling,* **30**(1), 67-84.

ZENKOUR, A.M., 2007. Benchmark trigonometric and 3-D elasticity solutions for an exponentially graded thick rectangular plate. *Archives of Applied Mechanics,* **77**(1), 197-214.

ZHENG, L. and ZHONG, Z., 2009. Exact Solution for Axisymmetric Bending of Functionally Graded Circular Plate. *Tsinghua Science & Technology,* **14**(Supplement 2), 64-68.

ZHONG, Z. and SHANG, E.T., 2003. Three-dimensional exact analysis of a simply supported functionally gradient piezoelectric plate. *International Journal of Solids and Structures,* **40**(20), 5335-5352.

ZHONG, Z. and SHANG, E., 2008. Closed-form solutions of three-dimensional functionally graded plates. *Mechanics of Advanced Materials and Structures,* **15**(5), 355-363.

Appendix A

Substituting strain displacement relations (7) into constitutive equation (3c)

$$\sigma_{33} = c_{13}\frac{\partial u_1}{\partial x_1} + c_{13}\frac{\partial u_2}{\partial x_2} + c_{33}\frac{\partial u_3}{\partial x_3} \tag{A1}$$

Now differentiating (9a) with respect to x_1 and (9b) with respect to x_2 gives

$$\frac{\partial u_1}{\partial x_1} = \frac{\partial^2 \Phi}{\partial x_1 \partial x_2} - \frac{1}{c_{11}c_{33} - c_{13}^2}\left[c_{13}\Delta_2 - c_{33}\frac{\partial^2}{\partial x_3^2}\right]\frac{\partial^2 \Psi}{\partial x_1^2} \tag{A2}$$

$$\frac{\partial u_2}{\partial x_2} = -\frac{\partial^2 \Phi}{\partial x_1 \partial x_2} - \frac{1}{c_{11}c_{33} - c_{13}^2}\left[c_{13}\Delta_2 - c_{33}\frac{\partial^2}{\partial x_3^2}\right]\frac{\partial^2 \Psi}{\partial x_2^2} \tag{A3}$$

Again referring to (Kashtalyan and Rushchitsky, 2009), the following relations were written

$$c_{33}u_{3,3} + c_{13}\Delta_2 F = \Delta_2\Delta_2\Psi \tag{A4}$$

$$F = -\frac{1}{c_{11}c_{33} - c_{13}^2}\left[c_{13}\Delta\Psi - (c_{13} + c_{33})\frac{\partial^2 \Psi}{\partial x_3^2}\right] \tag{A5}$$

where F is a displacement function $F = F(x_1, x_2, x_3)$ and Δ is the Laplacian operator.

Rearranging (A4)

$$c_{33}u_{3,3} = \Delta_2\Delta_2\Psi - c_{13}\Delta_2 F \tag{A6}$$

Now substituting (A5) into (A6)

$$c_{33}u_{3,3} = \Delta_2\Delta_2\Psi + c_{13}\Delta_2\left[\frac{c_{13}}{c_{11}c_{33} - c_{13}^2}\Delta\Psi - \frac{(c_{13} + c_{33})}{c_{11}c_{33} - c_{13}^2}\frac{\partial^2 \Psi}{\partial x_3^2}\right] \tag{A7}$$

Substituting $\Delta_2 = \Delta - \frac{\partial^2}{\partial x_3^2}$ and rearranging

$$u_{3,3} = \frac{1}{c_{11}c_{33} - c_{13}^2}\left[c_{11}\Delta - (c_{11} + c_{13})\frac{\partial^2}{\partial x_3^2}\right]\left(\Delta - \frac{\partial^2}{\partial x_3^2}\right)\Psi \tag{A8}$$

Now substituting (A2), (A3) and (A8) into (A1) yields

$$\sigma_{33} = c_{13}\frac{\partial^2\Phi}{\partial x_1\partial x_2} - \frac{c_{13}}{c_{11}c_{33}-c_{13}^2}\left[c_{13}\Delta_2 - c_{33}\frac{\partial^2}{\partial x_3^2}\right]\frac{\partial^2\Psi}{\partial x_1^2}$$
$$- c_{13}\frac{\partial^2\Phi}{\partial x_1\partial x_2} - \frac{c_{13}}{c_{11}c_{33}-c_{13}^2}\left[c_{13}\Delta_2 - c_{33}\frac{\partial^2}{\partial x_3^2}\right]\frac{\partial^2\Psi}{\partial x_2^2} \quad \text{(A9)}$$
$$+ \frac{c_{33}}{c_{11}c_{33}-c_{13}^2}\left[c_{11}\Delta - (c_{11}+c_{13})\frac{\partial^2}{\partial x_3^2}\right]\left(\Delta - \frac{\partial^2}{\partial x_3^2}\right)\Psi$$

After simplification

$$\sigma_{33} = \left(\Delta - \frac{\partial^2}{\partial x_3^2}\right)\left(\Delta - \frac{\partial^2}{\partial x_3^2}\right)\Psi \quad \text{(A10)}$$

or

$$\sigma_{33} = \Delta_2\Delta_2\Psi \quad \text{(A11)}$$

Derivation of other stress components, equations (9d, e, g-i), is carried out in a similar manner.

Appendix B

From Polyanin and Zaitsev (2003), a fourth order equation with constant coefficients has general solution

$$\widehat{\Psi} = C_1 \exp(\lambda_1 x_3) + C_2 \exp(\lambda_2 x_3) + C_3 \exp(\lambda_3 x_3) + C_4 \exp(\lambda_4 x_3) \tag{B1}$$

Begin by substituting $\widehat{\Psi} = \exp(\lambda x_3)$ and its derivatives into equation (15b) and simplifying, thus giving the following characteristic equation

$$\begin{aligned} &h^4\lambda^4 - 2\alpha h^3\lambda^3 + h^2\left[\alpha^2 + \left(2\frac{c_{13}^0}{c_{33}^0} - \frac{c_{11}^0 c_{33}^0 - c_{13}^{0\,2}}{c_{33}^0 c_{44}^0}\right)k_\Psi^2 h^2\right]\lambda^2 \\ &-\alpha k_\Psi^2 h^3\left(2\frac{c_{13}^0}{c_{33}^0} - \frac{c_{11}^0 c_{33}^0 - c_{13}^{0\,2}}{c_{33}^0 c_{44}^0}\right)\lambda + \frac{k_\Psi^2 h^2\left(c_{11}^0 k_\Psi^2 h^2 + c_{13}^0\alpha^2\right)}{c_{33}^0} = 0 \end{aligned} \tag{B2}$$

Comparing (B2) with

$$Ax^4 + Bx^3 + Cx^2 + Dx + E = 0, \tag{B3}$$

dividing by A and applying the change of variable $x = y - \frac{B}{4A}$ gives

$$\begin{aligned} &y^4 + \left(-\frac{3}{8}\frac{B^2}{A^2} + \frac{C}{A}\right)y^2 + \left(\frac{1}{8}\frac{B^3}{A^3} - \frac{BC}{2A^2} + \frac{D}{A}\right)y \\ &+\left(-\frac{3}{256}\frac{B^4}{A^4} + \frac{CB^2}{16A^3} - \frac{BD}{4A^2} + \frac{E}{A}\right) = 0 \end{aligned} \tag{B4}$$

Thus we have a depressed quadratic expression (i.e. no cubed term), which can be re-written as

$$y^4 + \theta y^2 + \kappa y + \phi = 0 \tag{B5}$$

where

$$\theta = -\frac{3}{8}\frac{B^2}{A^2} + \frac{C}{A} \tag{B6}$$

$$\kappa = \frac{1}{8}\frac{B^3}{A^3} - \frac{BC}{2A^2} + \frac{D}{A} \tag{B7}$$

and

$$\phi = -\frac{3}{256}\frac{B^4}{A^4} + \frac{CB^2}{16A^3} - \frac{BD}{4A^2} + \frac{E}{A} \tag{B8}$$

Comparing equations (B2) and (B5) it can be seen that

$$A = h^4 \tag{B9}$$

$$B = -2\alpha h^3 \tag{B10}$$

$$C = h^2\left[\alpha^2 + \left(2\frac{c_{13}^0}{c_{33}^0} - \frac{c_{11}^0 c_{33}^0 - c_{13}^{0\,2}}{c_{33}^0 c_{44}^0}\right)k_\Psi^2 h^2\right] \tag{B11}$$

$$D = -\alpha k_\Psi^2 h^3\left(2\frac{c_{13}^0}{c_{33}^0} - \frac{c_{11}^0 c_{33}^0 - c_{13}^{0\,2}}{c_{33}^0 c_{44}^0}\right) \tag{B12}$$

and

$$E = \frac{k_\Psi^2 h^2\left(c_{11}^0 k_\Psi^2 h^2 + c_{13}^0 \alpha^2\right)}{c_{33}^0} \tag{B13}$$

Substituting equations (B9-B12) into (B7) shows that

$$\kappa = 0 \tag{B14}$$

Substituting equations (B9-B11) into (B6)

$$\theta = -\frac{\alpha^2}{2h^2} + 2\frac{c_{13}^0 k_\Psi^2}{c_{33}^0} - \frac{c_{11}^0 k_\Psi^2}{c_{44}^0} + \frac{c_{13}^{0\,2} k_\Psi^2}{c_{33}^0 c_{44}^0} \tag{B15}$$

and substituting equations (B9-B13) into (B8) yields

$$\phi = \frac{\alpha^4}{16h^4} + \frac{1}{2}\frac{\alpha^2 c_{13}^0 k_\Psi^2}{h^2 c_{33}^0} + \frac{1}{4}\frac{\alpha^2 c_{11}^0 k_\Psi^2}{h^2 c_{44}^0} - \frac{1}{4}\frac{\alpha^2 c_{13}^{0\,2} k_\Psi^2}{h^2 c_{33}^0 c_{44}^0} + \frac{c_{11}^0 k_\Psi^4}{c_{33}^0} \tag{B16}$$

Therefore equation (B5) reduces to the following bi-quadratic

$$y^4 + \theta y^2 + \phi = 0 \tag{B17}$$

Making the change of variable $z = y^2$, (B17) can be rewritten as

$$z^2 + \theta z + \phi = 0 \tag{B18}$$

Now considering the discriminant of (B18)

$$Disc = \theta^2 - 4\phi$$
$$= -\frac{4\alpha^2 c_{13}^0 k_\Psi^2}{h^2 c_{33}^0} - 4\frac{c_{11}^0 k_\Psi^4}{c_{33}^0} + 4\frac{{c_{13}^0}^2 k_\Psi^4}{{c_{33}^0}^2} - 4\frac{c_{11}^0 c_{13}^0 k_\Psi^4}{c_{33}^0 c_{44}^0} + 4\frac{{c_{13}^0}^2 k_\Psi^4}{{c_{33}^0}^2 c_{44}^0} \quad \text{(B19)}$$
$$+ \frac{{c_{11}^0}^2 k_\Psi^4}{{c_{44}^0}^2} - 2\frac{c_{11}^0 {c_{13}^0}^2 k_\Psi^4}{c_{33}^0 {c_{44}^0}^2} + \frac{{c_{13}^0}^2 k_\Psi^4}{{c_{33}^0}^2 {c_{44}^0}^2}$$

Depending on the values of the constants $c_{11}^0, c_{13}^0, c_{33}^0, c_{44}^0, \alpha$ and k_Ψ this discriminant can be either positive of negative.

If the discriminant is negative, the equation (B18) has two complex conjugate roots. Using the quadratic formula, the roots of (B18) can be written as

$$z^+ = -\frac{\theta}{2} + \frac{i\sqrt{4\phi - \theta^2}}{2} \quad \text{(B20)}$$

and

$$z^- = -\frac{\theta}{2} - \frac{i\sqrt{4\phi - \theta^2}}{2} \quad \text{(B21)}$$

Thus the required solutions to (B17) are

$$y_1 = +\sqrt{z^+},\ y_2 = -\sqrt{z^+},\ y_3 = +\sqrt{z^-} \text{ and } y_4 = -\sqrt{z^-} \quad \text{(B22)}$$

To calculate these square roots, the following equation is employed

$$\sqrt{a \pm bi} = \sqrt{\frac{\sqrt{a^2 + b^2} + a}{2}} \pm i\sqrt{\frac{\sqrt{a^2 + b^2} - a}{2}} \quad \text{(B23)}$$

with

$$a = -\frac{\theta}{2} \text{ and } b = \frac{\sqrt{4\phi - \theta^2}}{2} \quad \text{(B24)}$$

so that

$$\sqrt{z} = \frac{\lambda}{h} \pm i\frac{\mu}{h} \quad \text{(B25)}$$

where

$$\lambda = \sqrt{\frac{\sqrt{a^2 + b^2} + a}{2}} \quad \text{(B26)}$$

and

$$\mu = \sqrt{\frac{\sqrt{a^2+b^2}-a}{2}} \tag{B27}$$

Substituting (B15, B16) into (B24) and this into (B26, B27) gives

$$\lambda = \frac{1}{4}\left[8\left(-\frac{c_{13}^0}{c_{33}^0} + \frac{1}{2}\frac{c_{11}^0}{c_{44}^0} - \frac{1}{2}\frac{c_{13}^{0^2}}{c_{33}^0 c_{44}^0} \right) k_\Psi^2 h^2 + 2\alpha^2 + 4\left(2\alpha^2 h^2 k_\Psi^2 \frac{c_{13}^0}{c_{33}^0} + \alpha^2 h^2 k_\Psi^2 \frac{c_{11}^0}{c_{44}^0} \right.\right.$$
$$\left.\left. - \alpha^2 h^2 k_\Psi^2 \frac{c_{13}^{0^2}}{c_{33}^0 c_{44}^0} + 4h^4 k_\Psi^4 \frac{c_{13}^0}{c_{33}^0} + \frac{1}{4}\alpha^4 \right)^{\frac{1}{2}} \right]^{\frac{1}{2}} \tag{B28}$$

and

$$\mu = \frac{1}{4}\left[8\left(\frac{c_{13}^0}{c_{33}^0} - \frac{1}{2}\frac{c_{11}^0}{c_{44}^0} + \frac{1}{2}\frac{c_{13}^{0^2}}{c_{33}^0 c_{44}^0} \right) k_\Psi^2 h^2 - 2\alpha^2 + 4\left(2\alpha^2 h^2 k_\Psi^2 \frac{c_{13}^0}{c_{33}^0} + \alpha^2 h^2 k_\Psi^2 \frac{c_{11}^0}{c_{44}^0} \right.\right.$$
$$\left.\left. - \alpha^2 h^2 k_\Psi^2 \frac{c_{13}^{0^2}}{c_{33}^0 c_{44}^0} + 4h^4 k_\Psi^4 \frac{c_{13}^0}{c_{33}^0} + \frac{1}{4}\alpha^4 \right)^{\frac{1}{2}} \right]^{\frac{1}{2}} \tag{B29}$$

Making the substitution $x = y - \frac{B}{4A}$, the roots of equation (B3) are found to be

$$\begin{aligned} x &= \pm\frac{\lambda}{h} \pm i\frac{\mu}{h} - \frac{B}{4A} \\ &= \pm\frac{\lambda}{h} \pm i\frac{\mu}{h} + \frac{\alpha}{2h} \end{aligned} \tag{B30}$$

Substituting the roots (B30) into general solution (B1), taking common factors and substituting trigonometric identities allows the solution of (15b) to be written

$$\begin{aligned} \hat{\Psi}(x_3) = h^4 \exp\left(\frac{\alpha x_3}{2h}\right)\left[A_1 \cosh\frac{\lambda x_3}{h}\cos\frac{\mu x_3}{h} + A_2 \cosh\frac{\lambda x_3}{h}\sin\frac{\mu x_3}{h} \right. \\ \left. + A_3 \sinh\frac{\lambda x_3}{h}\cos\frac{\mu x_3}{h} + A_4 \sinh\frac{\lambda x_3}{h}\sin\frac{\mu x_3}{h} \right] \end{aligned} \tag{B31}$$

If discriminant (B19) is positive, function $\hat{\Psi}$ is sought in a similar fashion.

Appendix C

Functions $U_{i,j}$ and $P_{rt,j}$ involved in Eqs. (19)

$$U_{1,j}(x_3) = -\frac{q_{mn}h}{c_{11}^0 c_{33}^0 - c_{13}^{0\,2}} \frac{\pi m h}{a} \exp\left(\frac{-\alpha x_3}{h}\right)\left[c_{13}^0 k_\Psi^2 h^2 f_j(x_3) + c_{33}^0 h^2 \frac{d^2}{dx_3^{\,2}} f_j(x_3)\right]$$

$$U_{2,j}(x_3) = -\frac{q_{mn}h}{c_{11}^0 c_{33}^0 - c_{13}^{0\,2}} \frac{\pi n h}{b} \exp\left(\frac{-\alpha x_3}{h}\right)\left[c_{13}^0 k_\Psi^2 h^2 f_j(x_3) + c_{33}^0 h^2 \frac{d^2}{dx_3^{\,2}} f_j(x_3)\right]$$

$$U_{3,j}(x_3) = -\frac{q_{mn}h}{c_{11}^0 c_{33}^0 - c_{13}^{0\,2}} \exp\left(\frac{-\alpha x_3}{h}\right)\left[c_{33}^0\left(-h^3 \frac{d^3}{dx_3^{\,3}} f_j(x_3) - \alpha \frac{d^2}{dx_3^{\,2}} f_j(x_3)\right)\right.$$
$$\left. + k_\Psi^2 h^2\left(h\left(\frac{c_{11}^0 c_{33}^0}{c_{44}^0} - c_{13}^0 - \frac{c_{13}^{0\,2}}{c_{44}^0}\right)\frac{d}{dx_3} f_j(x_3) + \alpha c_{13}^0 f_j(x_3)\right)\right], \quad j = 1,\ldots,4;$$

$$U_{1,j}(x_3) = -\frac{q_{mn}h}{c_{44}^0}\frac{\pi n h}{b} f_j(x_3), \qquad U_{2,j}(x_3) = \frac{q_{mn}h}{c_{44}^0}\frac{\pi m h}{a} f_j(x_3),$$

$$U_{3,j}(x_3) = 0, \quad j = 5,6;$$

$$P_{33,j}(x_3) = q_{mn} k_\Psi^4 h^4 f_j(x_3), \qquad P_{13,j}(x_3) = q_{mn} k_\Psi^2 h^3 \left(\frac{\pi m h}{a}\right)\frac{d}{dx_3} f_j(x_3)$$

$$P_{23,j}(x_3) = q_{mn} k_\Psi^2 h^3 \left(\frac{\pi n h}{b}\right)\frac{d}{dx_3} f_j(x_3)$$

$$P_{11,j}(x_3) = q_{mn}\left[\frac{c_{11}^0 c_{33}^0 - c_{12}^0 c_{13}^0}{c_{11}^0 c_{33}^0 - c_{13}^{0\,2}} k_\Psi^2 h^2 \left(\frac{\pi n h}{b}\right)^2 f_j(x_3)\right.$$
$$\left. - \frac{c_{12}^0 c_{33}^0 - c_{13}^{0\,2}}{c_{11}^0 c_{33}^0 - c_{13}^{0\,2}} h^2 \left(\frac{\pi n h}{b}\right)^2 \frac{d^2}{dx_3^2} f_j(x_3) - h^2 \left(\frac{\pi m h}{a}\right)^2 \frac{d^2}{dx_3^2} f_j(x_3)\right]$$

$$P_{22,j}(x_3) = q_{mn}\left[\frac{c_{11}^0 c_{13}^0 - c_{12}^0 c_{13}^0}{c_{11}^0 c_{33}^0 - c_{13}^{0\,2}} k_\Psi^2 h^2 \left(\frac{\pi m h}{a}\right)^2 f_j(x_3)\right.$$
$$\left. - \frac{c_{12}^0 c_{33}^0 - c_{13}^{0\,2}}{c_{11}^0 c_{33}^0 - c_{13}^{0\,2}} h^2 \left(\frac{\pi m h}{a}\right)^2 \frac{d^2}{dx_3^2} f_j(x_3) - h^2 \left(\frac{\pi n h}{b}\right)^2 \frac{d^2}{dx_3^2} f_j(x_3)\right]$$

$$P_{12,j}(x_3) = q_{mn} \frac{c_{11}^0 - c_{12}^0}{c_{11}^0 c_{33}^0 - c_{13}^{0\,2}} \left(\frac{\pi m h}{a}\right)\left(\frac{\pi n h}{b}\right) h^2 \left[c_{13}^0 k_\Psi^2 f_j(x_3) + c_{33}^0 \frac{d^2}{dx_3^2} f_j(x_3)\right], \quad j = 1,\ldots,4;$$

$$P_{33,j}(x_3)=0\,,\qquad P_{13,j}(x_3)=-q_{mn}\left(\frac{\pi nh}{b}\right)\exp\left(\frac{\alpha x_3}{h}\right)\frac{d}{dx_3}\,f_j(x_3)$$

$$P_{23,j}(x_3)=q_{mn}\left(\frac{\pi mh}{a}\right)\exp\left(\frac{\alpha x_3}{h}\right)\frac{d}{dx_3}\,f_j(x_3)$$

$$P_{11,j}(x_3)=\frac{q_{mn}}{c_{44}^0}\frac{1}{c_{11}^0c_{33}^0-c_{13}^{0\,2}}\left(\frac{\pi nh}{b}\right)\left(\frac{\pi mh}{a}\right)\exp\left(\frac{\alpha x_3}{h}\right)\times$$
$$\left(c_{12}^0c_{13}^{0\,2}+c_{11}^{0\,2}c_{33}^0-c_{11}^0c_{13}^{0\,2}-c_{12}^0c_{11}^0c_{33}^0\right)f_j(x_3)$$

$$P_{22,j}(x_3)=\frac{q_{mn}}{c_{44}^0}\frac{1}{c_{11}^0c_{33}^0-c_{13}^{0\,2}}\left(\frac{\pi nh}{b}\right)\left(\frac{\pi mh}{a}\right)\exp\left(\frac{\alpha x_3}{h}\right)\times$$
$$\left(-c_{12}^0c_{13}^{0\,2}-c_{11}^{0\,2}c_{33}^0+c_{11}^0c_{13}^{0\,2}+c_{12}^0c_{11}^0c_{33}^0\right)f_j(x_3)$$

$$P_{12,j}(x_3)=\frac{q_{mn}}{2}\frac{c_{11}^0-c_{12}^0}{c_{44}^0}\left[\left(\frac{\pi mh}{a}\right)^2-\left(\frac{\pi nh}{b}\right)^2\right]\exp\left(\frac{\alpha x_3}{h}\right)f_j(x_3)\qquad j=5,6\,.$$

In the expressions above, functions $f_j(x_3)$ $(j=1,\ldots,6)$ are

$$f_1(x_3)=\exp\left(\frac{\alpha x_3}{2h}\right)\cosh\frac{\lambda x_3}{h}\cos\frac{\mu x_3}{h}\,,$$

$$f_2(x_3)=\exp\left(\frac{\alpha x_3}{2h}\right)\sinh\frac{\lambda x_3}{h}\cos\frac{\mu x_3}{h}$$

$$f_3(x_3)=\exp\left(\frac{\alpha x_3}{2h}\right)\cosh\frac{\lambda x_3}{h}\sin\frac{\mu x_3}{h}\,,$$

$$f_4(x_3)=\exp\left(\frac{\alpha x_3}{2h}\right)\sinh\frac{\lambda x_3}{h}\sin\frac{\mu x_3}{h}\,;$$

$$f_5(x_3)=\exp\left(-\frac{\alpha x_3}{2h}\right)\cosh\frac{\beta x_3}{h}\,;$$

$$f_6(x_3)=\exp\left(-\frac{\alpha x_3}{2h}\right)\sinh\frac{\beta x_3}{h}\,.$$

Tables

Table 1. Normalised displacements and stresses in a square simply supported isotropic graded plate with $a/h=3, \quad \alpha=2.3$

	Kashtalyan (2004)	Present solution	Difference, %
$\frac{c_{44}^0 u_3}{q_{11} h}(0.5a, 0.5a, 0.5h)$	-4.29778	-4.30352	0.001333
$\frac{\sigma_{11}}{q_{11}}(0.5a, 0.5a, 0.5h)$	0.653339	0.652648	0.001059
$\frac{\sigma_{12}}{q_{11}}(0., 0., 0.5h)$	-0.43007	-0.42974	0.000774
$\frac{\sigma_{13}}{q_{11}}(0.,0.5a, 0.5h)$	-0.64606	-0.64618	0.000188

Table 2. Normalised displacement $\frac{G_2 u_3(0.5a, 0.5a, 0.5h)}{q_{11}h}$ in a square simply supported isotropic graded plate under sinusoidal loading with the shear modulus varying exponentially from G_1 at the bottom surface to G_2 at the top surface ($G_2/G_1 = 10$).

h/a	Present 3-D solution	Thin plate theory (Chi and Chung, 2006)	Difference (%)
0.001	3.52725E+11	3.52724E+11	0.000491
0.01	35289681.36	35272367.69	0.049062
0.02	2208851.489	2204522.98	0.195962
0.04	138864.9234	137782.6863	0.779345
0.06	27697.41125	27216.33309	1.736907
0.08	8882.100634	8611.417892	3.047508
0.1	3700.547069	3527.236769	4.68337
0.15	773.9162053	696.7381272	9.972408
0.2	264.0397906	220.452298	16.50793

Table 3. Normalised displacement $\frac{G_2 u_3(0.5a, 0.5a, 0.5h)}{q_{11}h}$ in a square simply supported isotropic graded plate under sinusoidal loading with the shear modulus varying exponentially from G_1 at the bottom surface to G_2 at the top surface ($a/h = 100$).

G_2/G_1	Present 3-D solution	Thin plate theory (Chi and Chung, 2006)	Difference (%)
1.5	1983989.7	1982974.631	0.051161
2	3062381.7	3060801.301	0.051607
3	5657499.8	5654572.722	0.051737
4	8755021.8	8750513.815	0.051491
5	12290237	12283954.61	0.051118
10	35289681	35272367.69	0.049062
20	101163976	101117511.8	0.045929

Table 4. Normalised displacement $\frac{10E_0h^3u_3(0.5a,0.5b,0.5h)}{a^4q_{11}}$ in a simply supported isotropic graded plate under sinusoidal loading with the Young's modulus varying exponentially from E_0 at the bottom surface to $E_0 \exp k$ at the top surface.

a/b	Theory	$k=0.1$	Difference (%)	$k=0.3$	Difference (%)	$k=0.5$	Difference (%)	$k=0.7$	Difference (%)	$k=1.$	Difference (%)	$k=1.5$	Difference (%)
$a/h=2$													
1	TPT	0.5731	0.0255	0.5181	-0.6557	0.4679	-1.3744	0.4222	-2.1303	0.3612	-3.3318	0.2771	-5.5080
	HPT	0.5859	-2.2040	0.5296	-2.8881	0.4781	-3.5974	0.4313	-4.3342	0.3687	-5.4890	0.2825	-7.5411
	Present	0.5732		0.5147		0.4615		0.4134		0.3495		0.2627	
1/6	TPT	1.6294	-0.0011	1.4731	-0.4983	1.3307	-0.9812	1.2010	-1.4515	1.0282	-2.1321	0.7906	-3.2221
	HPT	1.5478	5.0082	1.3996	4.5127	1.2649	4.0069	1.1425	3.4918	0.9796	2.7022	0.7556	1.3426
	Present	1.6294		1.4658		1.3177		1.1838		1.0068		0.7659	
$a/h=4$													
1	TPT	0.3475	0.1066	0.3142	-0.1595	0.2839	-0.3692	0.2563	-0.5218	0.2196	-0.6520	0.1692	-0.6599
	HPT	0.3111	10.5648	0.2815	10.2743	0.2546	9.9795	0.2303	9.6908	0.1980	9.2523	0.1538	8.5305
	Present	0.3479		0.3137		0.2828		0.2550		0.2182		0.1681	
1/6	TPT	1.1668	0.1999	1.0551	0.0927	0.9535	0.0699	0.8611	0.1272	0.7382	0.3498	0.5697	1.0175
	HPT	1.0065	13.9125	0.9109	13.7490	0.8245	13.5871	0.7464	13.4274	0.6431	13.1940	0.5018	12.8167
	Present	1.1691		1.0561		0.9541		0.8622		0.7408		0.5755	

Table 5. Properties of Beryl rock

c_{11}^0 (GPa)	c_{12}^0 (GPa)	c_{13}^0 (GPa)	c_{33}^0 (GPa)	c_{44}^0 (GPa)	g^0
41.3	14.7	10.1	36.2	10.0	0.75

Figure captions

Fig.1: Schematic of the plate showing its geometry and applied loading.

Fig. 2: Through thickness variation of constant c_{11} for different values of α.

Fig. 3: Through-thickness variation of the normalised out of plane normal stress $\bar{\sigma}_{33}$ $(0.5a, 0.5b, x_3)$ in: (A) thick FG plate; (B) thin FG plate for a range of degrees of imhomogenity ($\alpha = 0, 2.3, 3$).

Fig. 4: Through-thickness variation of the normalised transverse shear stress $\bar{\sigma}_{13}$ $(0, 0.5b, x_3)$ in: (A) thick FG plate; (B) thin FG plate for a range of degrees of imhomogenity ($\alpha = 0, 2.3, 3$).

Fig. 5: Through-thickness variation of the normalised in-plane normal stress $\bar{\sigma}_{11}$ $(0.5a, 0.5b, x_3)$ in: (A) thick FG plate; (B) thin FG plate for a range of degrees of imhomogenity ($\alpha = 0, 2.3, 3$).

Fig. 6: Through-thickness variation of the normalised in-plane shear stress $\bar{\sigma}_{12}$ $(0, 0, x_3)$ in: (A) thick FG plate; (B) thin FG plate for a range of degrees of imhomogenity ($\alpha = 0, 2.3, 3$).

Fig. 7: Through-thickness variation of the normalised in-plane displacement $\bar{u}_1$ $(0, 0.5b, x_3)$ in: (A) thick FG plate; (B) thin FG plate for a range of degrees of imhomogenity ($\alpha = 0, 2.3, 3$).

Fig. 8: Through-thickness variation of the normalised transverse displacement $\bar{u}_3$ $(0.5a, 0.5b, x_3)$ in: (A) thick FG plate; (B) thin FG plate for a range of degrees of imhomogenity ($\alpha = 0, 2.3, 3$).

Fig. 9: Through-thickness variation of the normalised out of plane normal stress $\bar{\sigma}_{33}$ $(0.5a, 0.5b, x_3)$ in: (A) thick FG plate; (B) thin FG plate for a range of degrees of anisotropy ($g^0 = 0.038, 0.15, 0.75$).

Fig. 10: Through-thickness variation of the normalised transverse shear stress $\bar{\sigma}_{13}$ $(0, 0.5b, x_3)$ in: (A) thick FG plate; (B) thin FG plate for a range of degrees of anisotropy ($g^0 = 0.038, 0.15, 0.75$).

Fig. 11: Through-thickness variation of the normalised in-plane normal stress $\bar{\sigma}_{11}$ $(0.5a, 0.5b, x_3)$ in: (A) thick FG plate; (B) thin FG plate for a range of degrees of anisotropy ($g^0 = 0.038, 0.15, 0.75$).

Fig. 12: Through-thickness variation of the normalised in-plane shear stress $\bar{\sigma}_{12}$ $(0, 0, x_3)$ in: (A) thick FG plate; (B) thin FG plate for a range of degrees of anisotropy ($g^0 = 0.038, 0.15, 0.75$).

Fig. 13: Through-thickness variation of the normalised in-plane displacement $\bar{u}_1$ $(0, 0.5b, x_3)$ in: (A) thick FG plate; (B) thin FG plate for a range of degrees of anisotropy ($g^0 = 0.038, 0.15, 0.75$).

Fig. 14: Through-thickness variation of the normalised transverse displacement $\bar{u}_3$ $(0.5a, 0.5b, x_3)$ in: (A) thick FG plate; (B) thin FG plate for a range of degrees of anisotropy ($g^0 = 0.038, 0.15, 0.75$).

Figures

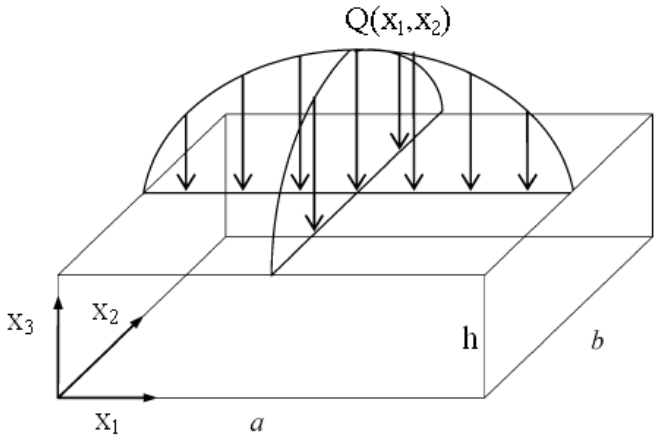

Fig. 1:

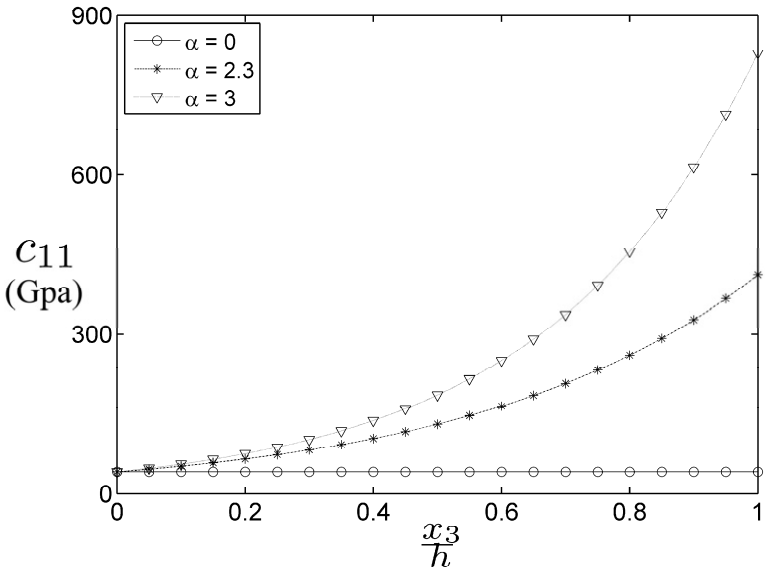

Fig. 2:

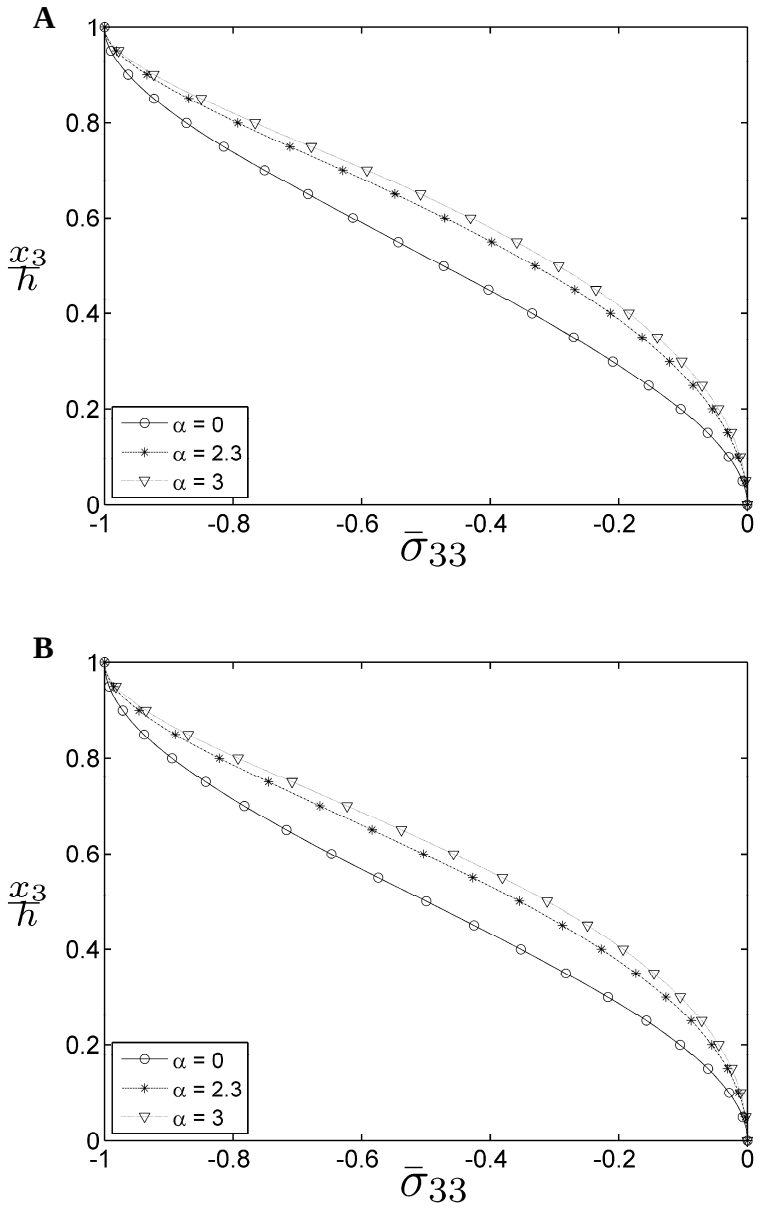

Fig. 3:

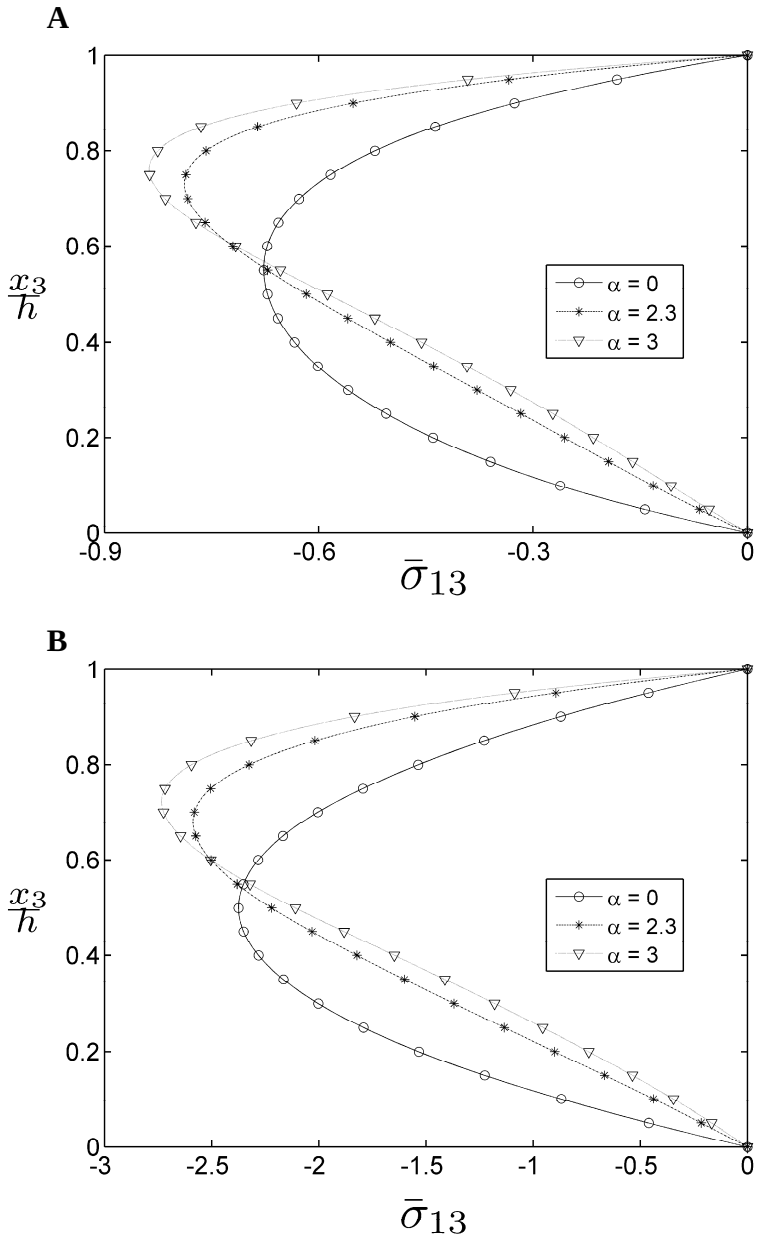
A
1
0.8
0.6
0.4
0.2
0
$\frac{x_3}{h}$
α = 0
α = 2.3
α = 3
-0.9
-0.6
-0.3
0
$\bar{\sigma}_{13}$
B
1
0.8
0.6
0.4
0.2
0
$\frac{x_3}{h}$
α = 0
α = 2.3
α = 3
-3
-2.5
-2
-1.5
-1
-0.5
0
$\bar{\sigma}_{13}$

Fig. 4:

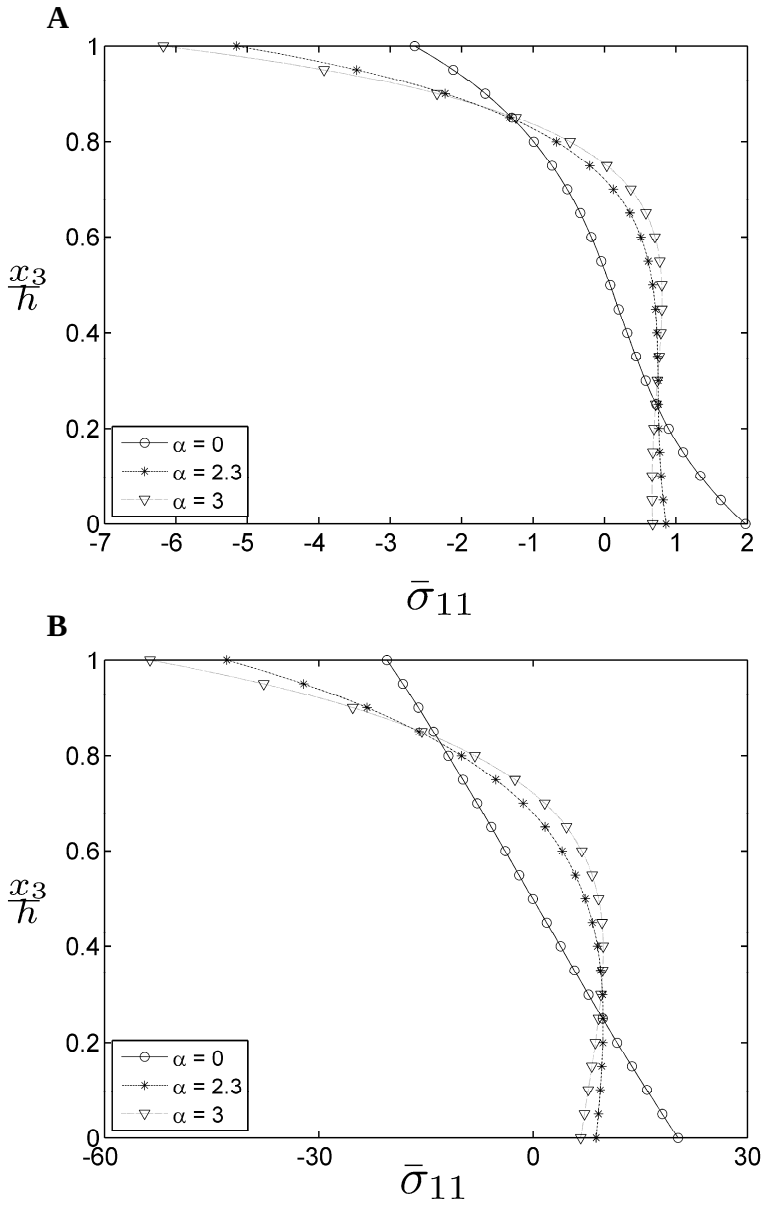
A
1
0.8
0.6
0.4
0.2
0
$\frac{x_3}{h}$
α = 0
α = 2.3
α = 3
-7
-6
-5
-4
-3
-2
-1
0
1
2
$\bar{\sigma}_{11}$
B
1
0.8
0.6
0.4
0.2
0
$\frac{x_3}{h}$
α = 0
α = 2.3
α = 3
-60
-30
0
30
$\bar{\sigma}_{11}$

Fig. 5:

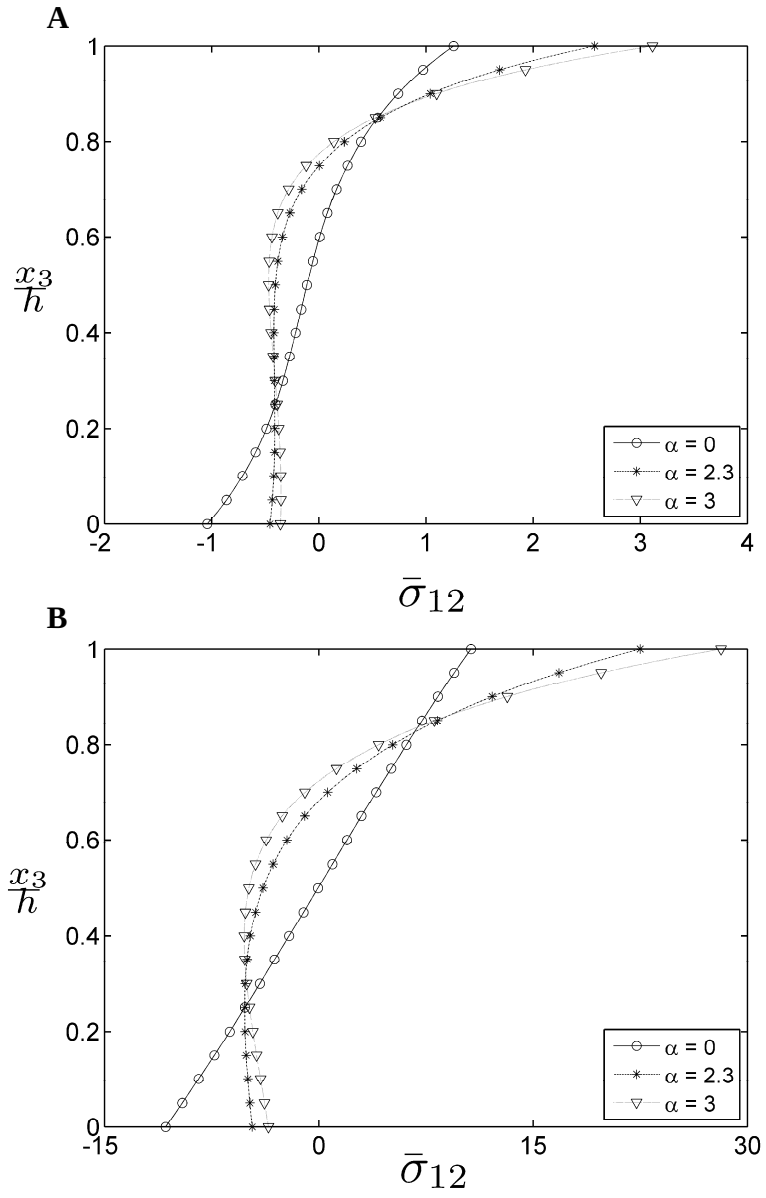
A
1
0.8
0.6
0.4
0.2
0
$\frac{x_3}{h}$
-2
-1
0
1
2
3
4
$\bar{\sigma}_{12}$
α = 0
α = 2.3
α = 3
B
1
0.8
0.6
0.4
0.2
0
$\frac{x_3}{h}$
-15
0
15
30
$\bar{\sigma}_{12}$
α = 0
α = 2.3
α = 3

Fig. 6:

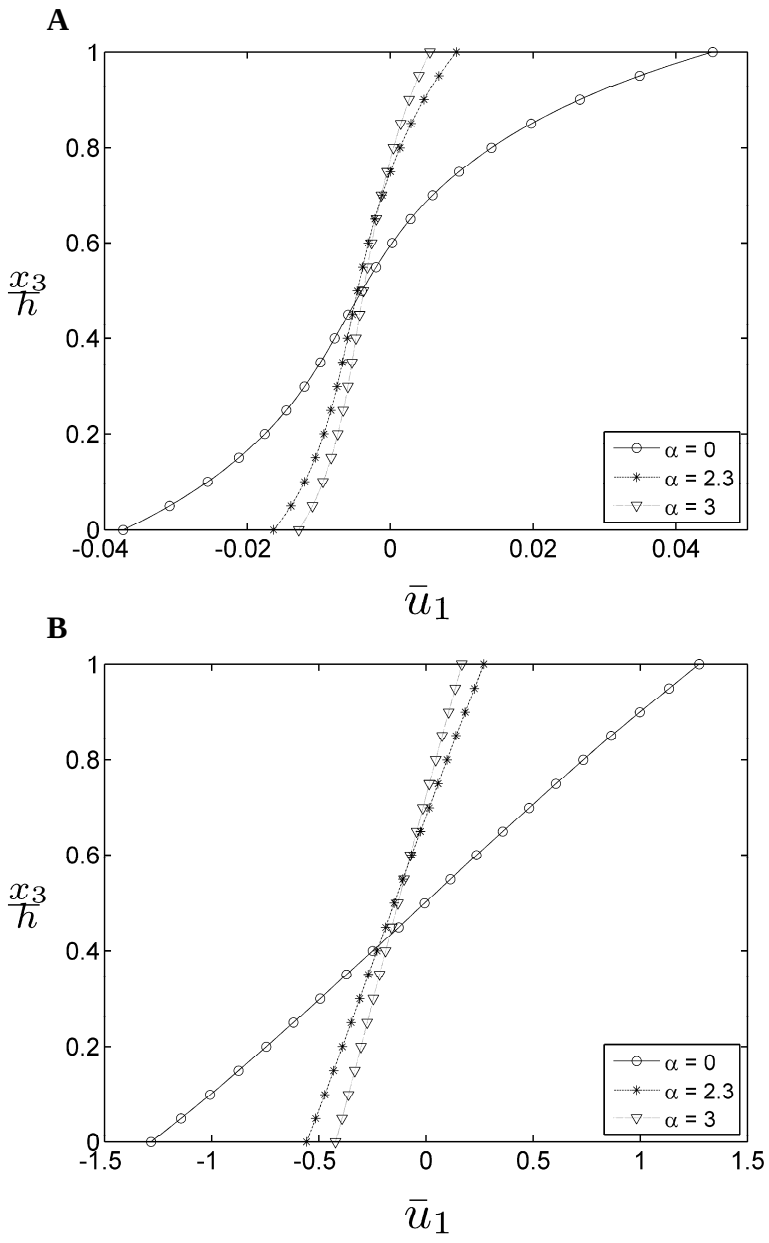
A
1
0.8
0.6
0.4
0.2
0
$\frac{x_3}{h}$
-0.04
-0.02
0
0.02
0.04
$\bar{u}_1$
α = 0
α = 2.3
α = 3
B
1
0.8
0.6
0.4
0.2
0
$\frac{x_3}{h}$
-1.5
-1
-0.5
0
0.5
1
1.5
$\bar{u}_1$
α = 0
α = 2.3
α = 3

Fig. 7:

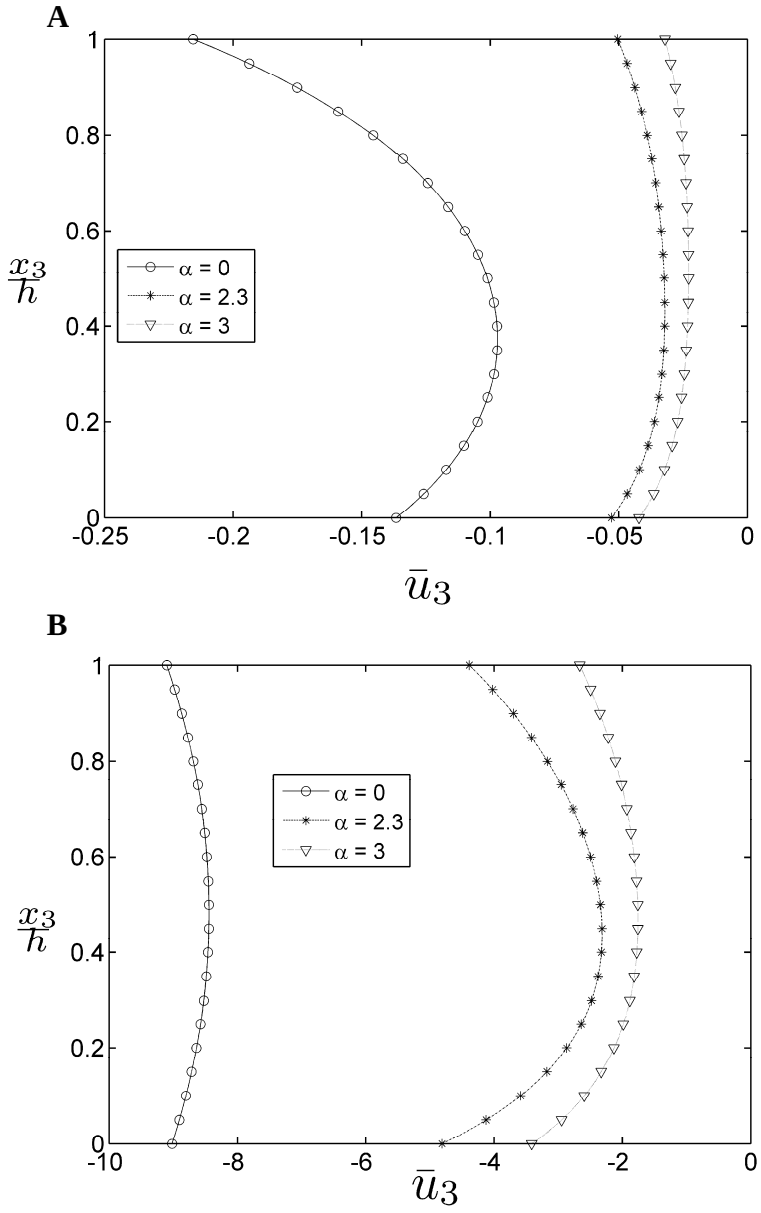
A
1
0.8
0.6
0.4
0.2
0
$\frac{x_3}{h}$
α = 0
α = 2.3
α = 3
-0.25
-0.2
-0.15
-0.1
-0.05
0
$\bar{u}_3$
B
1
0.8
0.6
0.4
0.2
0
$\frac{x_3}{h}$
α = 0
α = 2.3
α = 3
-10
-8
-6
-4
-2
0
$\bar{u}_3$

Fig. 8:

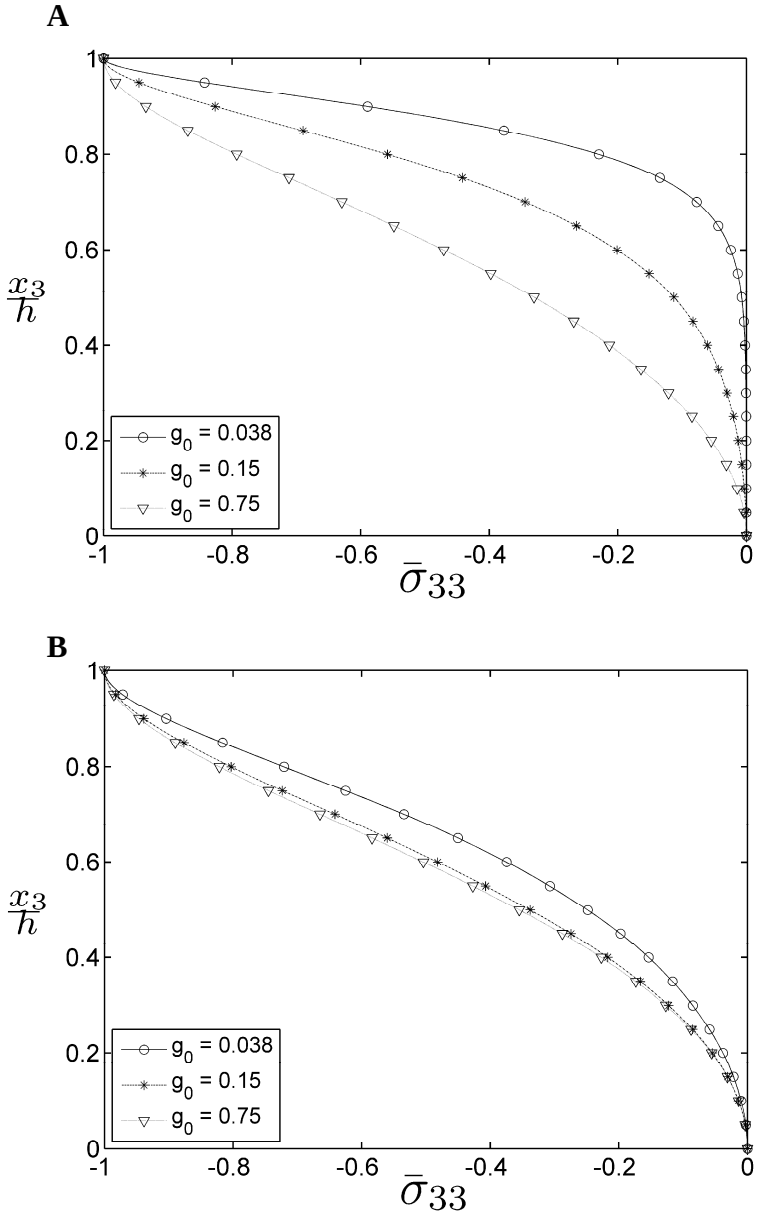
A
B
$\frac{x_3}{h}$
$\bar{\sigma}_{33}$
g_0 = 0.038
g_0 = 0.15
g_0 = 0.75
0
0.2
0.4
0.6
0.8
1
-1
-0.8
-0.6
-0.4
-0.2
0

Fig. 9:

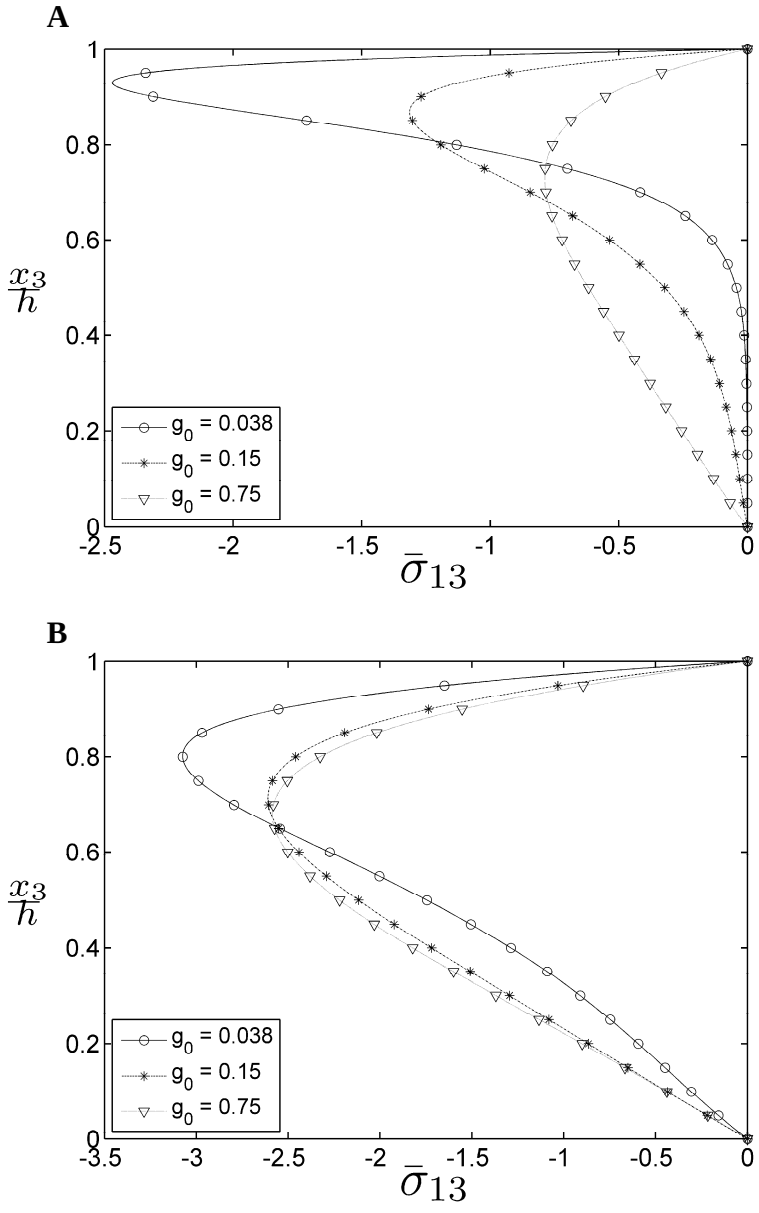

Fig. 10:

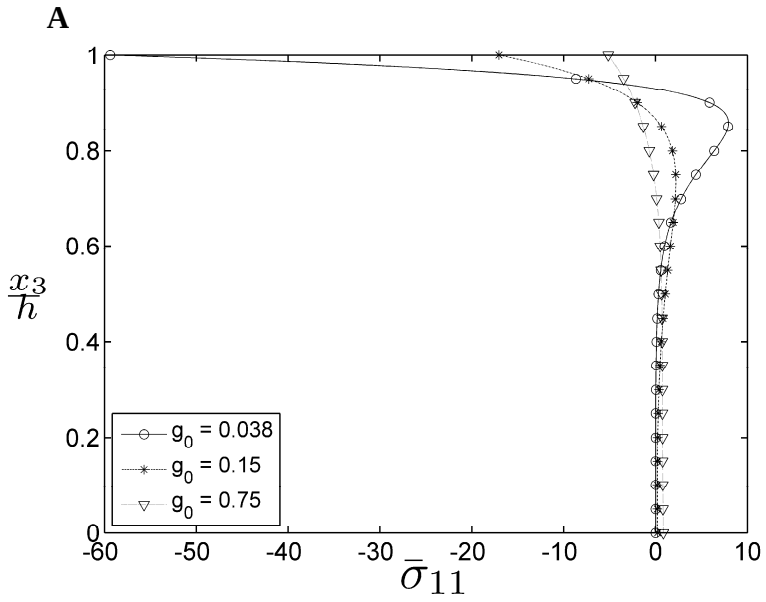
A
1
0.8
0.6
0.4
0.2
0
$\frac{x_3}{h}$
g_0 = 0.038
g_0 = 0.15
g_0 = 0.75
-60
-50
-40
-30
-20
-10
0
10
$\bar{\sigma}_{11}$

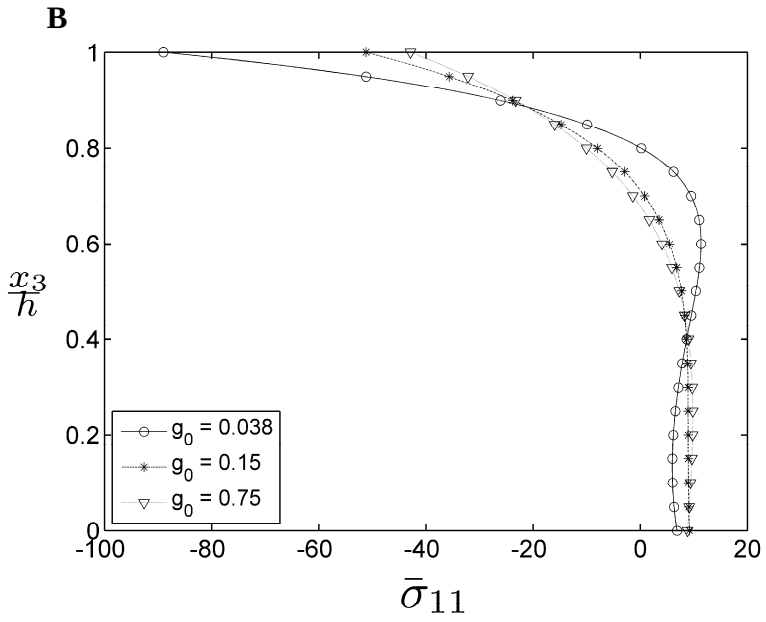
B
1
0.8
0.6
0.4
0.2
0
$\frac{x_3}{h}$
g_0 = 0.038
g_0 = 0.15
g_0 = 0.75
-100
-80
-60
-40
-20
0
20
$\bar{\sigma}_{11}$

Fig. 11:

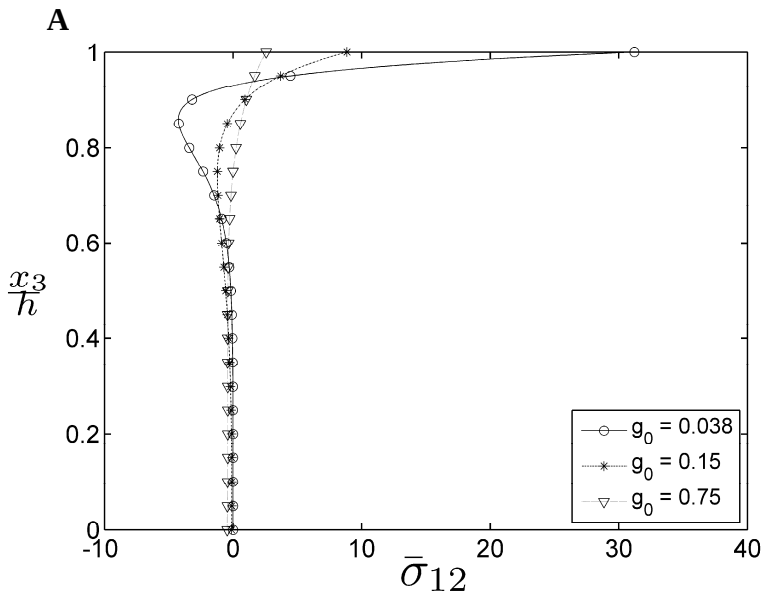
A
1
0.8
0.6
0.4
0.2
0
-10
0
10
20
30
40
$\frac{x_3}{h}$
$\bar{\sigma}_{12}$
g_0 = 0.038
g_0 = 0.15
g_0 = 0.75

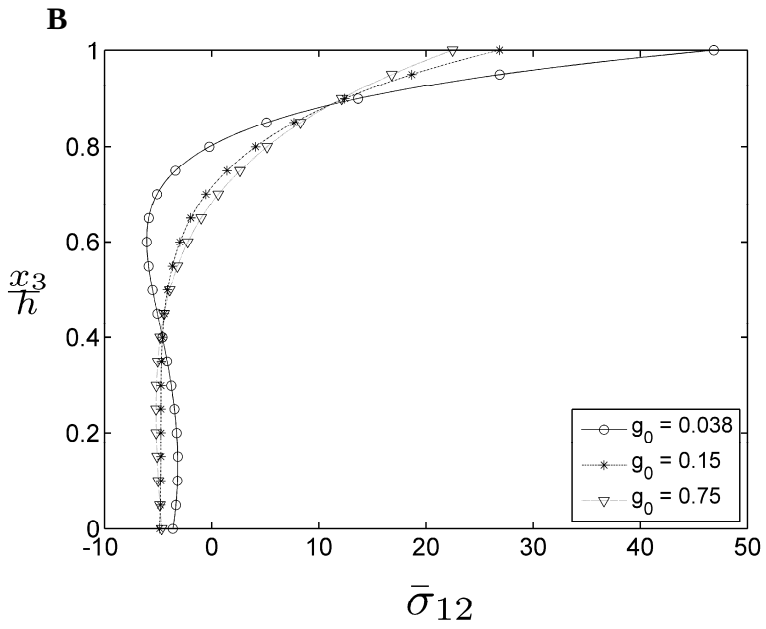
B
1
0.8
0.6
0.4
0.2
0
-10
0
10
20
30
40
50
$\frac{x_3}{h}$
$\bar{\sigma}_{12}$
g_0 = 0.038
g_0 = 0.15
g_0 = 0.75

Fig. 12:

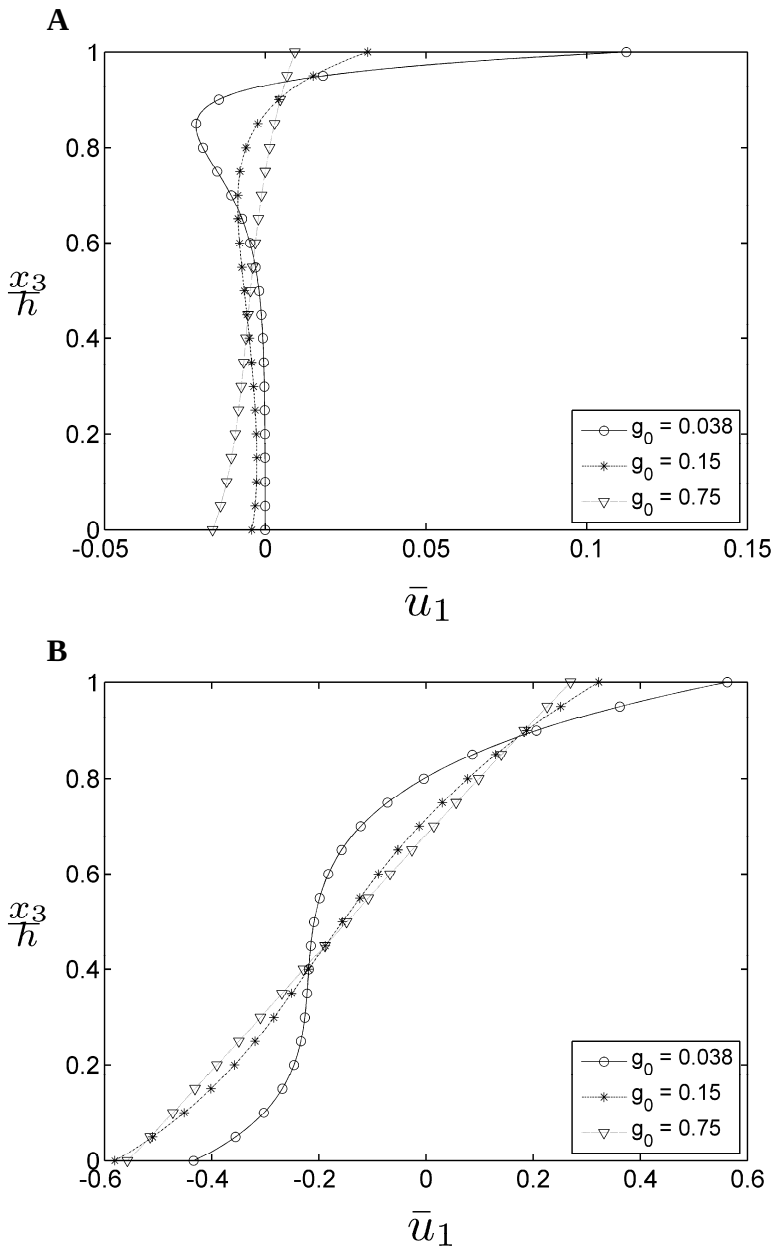
A
1
0.8
0.6
0.4
0.2
0
$\frac{x_3}{h}$
-0.05
0
0.05
0.1
0.15
$\bar{u}_1$
g_0 = 0.038
g_0 = 0.15
g_0 = 0.75
B
1
0.8
0.6
0.4
0.2
0
$\frac{x_3}{h}$
-0.6
-0.4
-0.2
0
0.2
0.4
0.6
$\bar{u}_1$
g_0 = 0.038
g_0 = 0.15
g_0 = 0.75

Fig. 13:

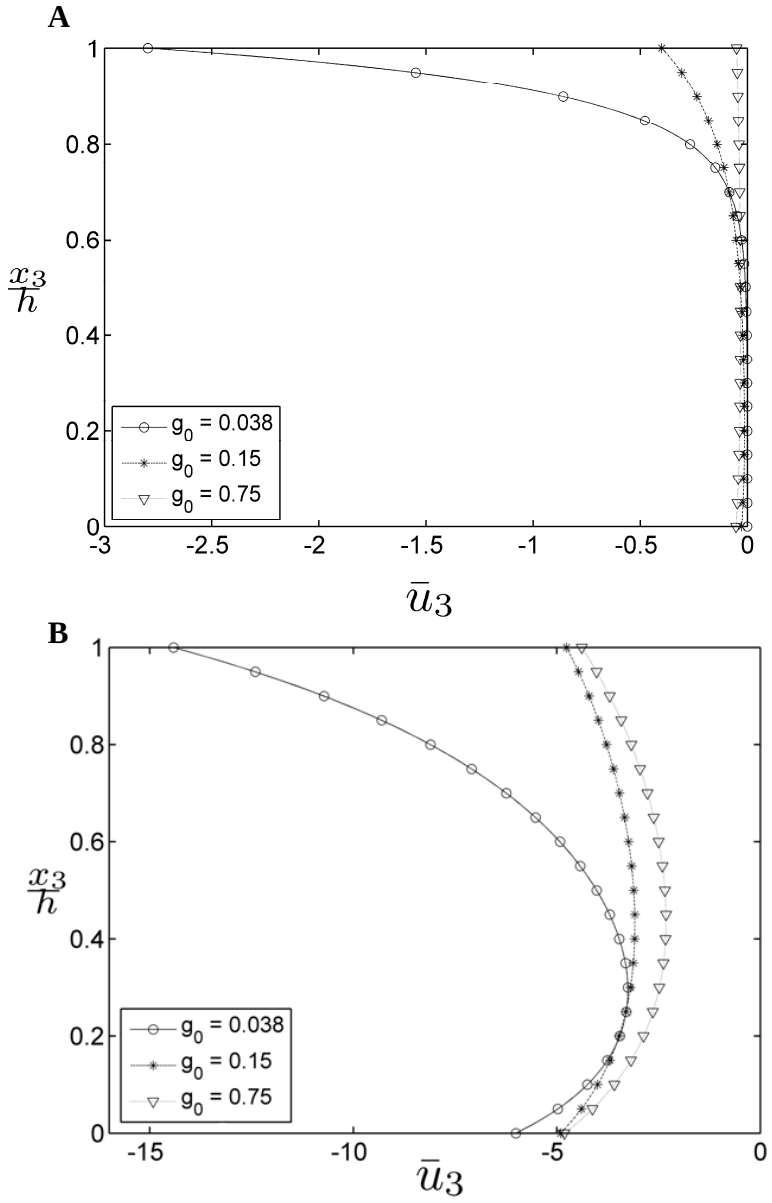
A
1
0.8
0.6
0.4
0.2
0
$\frac{x_3}{h}$
g_0 = 0.038
g_0 = 0.15
g_0 = 0.75
-3
-2.5
-2
-1.5
-1
-0.5
0
$\bar{u}_3$
B
1
0.8
0.6
0.4
0.2
0
$\frac{x_3}{h}$
g_0 = 0.038
g_0 = 0.15
g_0 = 0.75
-15
-10
-5
0
$\bar{u}_3$

Fig. 14: